Static strength prediction of adhesive joints: A review

L.D.C. Ramalho [b, *], R.D.S.G. Campilho [b, c], J. Belinha [c], L.F.M. da Silva [a]

[a] *Faculty of Engineering of the University of Porto, FEUP, Rua Dr. Roberto Frias, 4200-465, Porto, Portugal*
[b] *INEGI, Institute of Mechanical Engineering, Rua Dr. Roberto Frias, 4200-465, Porto, Portugal*
[c] *School of Engineering, Polytechnic of Porto, ISEP-IPP, Rua Dr. António Bernardino de Almeida, 431, 4200-072, Porto, Portugal*

ARTICLE INFO

ABSTRACT

The use of adhesive joints has gathered increasing interest in recent years due to their advantages over conventional bonding techniques, namely lighter structures and decreased stress concentrations. Consequentially, the strength prediction of adhesive joints has been studied extensively. This review aims to describe and compare the most relevant methods for the strength prediction of adhesive joints. These methods can be divided into analytical and numerical methods. Analytical methods are generally limited to initial design evaluations or to simple joints. Numerical methods are more commonly used, especially when joint design is complex. Between the different numerical methods, Cohesive Zone Models (CZM) are the most popular method to predict the strength of adhesive joints. This approach is able to predict the strength of a wide range of joint designs with minimal errors. However, it requires the determination of cohesive laws that generally change depending on different geometrical parameters of the joints. Advanced numerical techniques, such as the eXtended Finite Element Method (XFEM) or Meshless Methods have been used to study adhesive joints, but their application needs improvements before they can be more extensively used.

1. Introduction

Nowadays, adhesive joints are used in a wide range of engineering structures, including vehicles, airplanes and buildings, and each of those applications has different design needs. The use of adhesive joints has been increasing in recent years because of the advantages that they possess, including reduced stress concentrations and reduced weight, when compared to traditional mechanical bonding, such as bolted or riveted joints [1]. Due to their widespread and varied use, it is important to have accurate strength prediction techniques to aid in the design of adhesive joints. Some commonly studied adhesive joints are Single-Lap Joints (SLJ), Double-Lap Joints (DLJ), Strap Joints (SJ), Double-Strap Joints (DSJ), Scarf Joints (ScJ), single-L joints, T-joints and T-peel joints, represented in Fig. 1.

The main goal of this work is to provide a review of the developments in the strength prediction of adhesive joints that happened during the current decade. For older works, the review of He [2] can be consulted. Other reviews also discuss some strength prediction models for adhesive joints [3,4]. However, they are not focused on strength prediction methods, unlike the present work. This paper presents a general overview of the tests used to obtain the mechanical and fracture properties of adhesives, both in shear and tension, in Section 2. Section 3 discusses the recent papers focused on the strength prediction of adhesive joints, dividing the strength prediction methods into two groups, analytical methods and numerical methods. In the last section, Section 4, the conclusions of this work are presented.

2. Adhesive characterization tests

As the main goal of this paper is to review the different static strength prediction techniques employed in adhesive joints, it is important to mention which tests are performed to obtain the mechanical and fracture properties of adhesives. But, since experimental testing is not the main focus of this work, only a brief overview of the tests is presented. For detailed explanations on how to prepare the adhesive joints for testing and how to extract the adhesive properties from the tests, the book of da Silva et al. [5] and the review of Chaves et al. [6] can be consulted.

The tensile elastic modulus, and tensile yield and failure stresses, are generally obtained by loading bulk adhesive specimens in tension [7]. To determine the shear modulus and shear yield and failure stresses there are several alternative tests, examples of which include the Thick Adherend Shear Test (TAST) [8], Arcan [9] and Napkin Ring test [10],

---

Nomenclature

t_P	Adherend thickness
t_A	Adhesive thickness
ATDCB	Asymmetrical Tapered Double-Cantilever Beam
t_0	Cohesive strength
CZM	Cohesive Zone Models
CDM	Continuum Damage Model
CLS	Critical Longitudinal Strain
CNS	Critical Normal Strain
G_c	Critical strain energy release rate
δ^0	Displacement at peak traction
DCB	Double-Cantilever Beam
DLJ	Double-Lap Joints
DSJ	Double-Strap Joints
ENF	End-Notched Flexure
Γ_b	Energy expended in the bulk of the adhesive
XFEM	Extended Finite Element Method
FRP	Fibre Reinforced Polymer
FEA	Finite Element Analysis
FEM	Finite Element Method
FFM	Finite Fracture Mechanics
4ENF	Four-point ENF
FPZ	Fracture Process Zone
ICZM	Interpolation-Based CZM
MAXPE	Maximum Principal Strain
MAXPS	Maximum Principal Stress
MAXE	Maximum Strain
MAXS	Maximum Stress
MMB	Mixed Mode Bending
G_I	Mode I strain energy release rate
K_I	Mode I Stress Intensity Factor
G_{IIc}	Mode II critical strain energy release rate
G_{II}	Mode II strain energy release rate
K_{II}	Mode II Stress Intensity Factor
Γ_0	Intrinsic work of fracture
L_O	Overlap Length
QUADE	Quadratic strain
QUADS	Quadratic stress
RPIM	Radial Point Interpolation Method
ScJ	Scarf Joints
t_s^0	Shear cohesive strength
μ	Shear modulus
SLB	Single Leg Bending
SENB	Single-Edge Notched Bending
SLJ	Single-Lap Joints
SPH	Smoothed Particle Hydrodynamics
δ^s	Softening initiation displacement
SERR, G	Strain Energy Release Rate
SIF, K	Stress Intensity Factor
SJ	Strap Joints
TDCB	Tapered Double-Cantilever Beam
t_n^0	Tensile cohesive strength
E	Tensile modulus
TAST	Thick Adherend Shear Test
3D	Three-Dimensional
VCCT	Virtual Crack Closure Technique

represented in Fig. 2. A recent comparison between different tests used to obtain shear properties [8] showed that the Arcan and Napkin Ring tests are better than the other alternatives. These tests have almost constant shear stress along the adhesive length and their triaxiality ratio is 0, meaning that the stress at the adhesive layer is pure shear, unlike in the TAST. These tensile and shear tests are required to perform strength predictions of adhesive joints, regardless of the method used to predict it.

To determine the mode I critical strain energy release rate (G_{Ic}), several tests can be used, namely the Double-Cantilever Beam (DCB) [11], the Tapered Double-Cantilever Beam (TDCB) [12] and the Single-Edge Notched Bending (SENB) [13], shown in Fig. 3. A comparison between the DCB and the TDCB, performed by Teixeira et al. [14], showed that the TDCB underpredicts the G_{Ic} of ductile adhesives, making the DCB an overall better option to determine G_{Ic}. These tests are required to perform strength predictions of adhesive joints when using
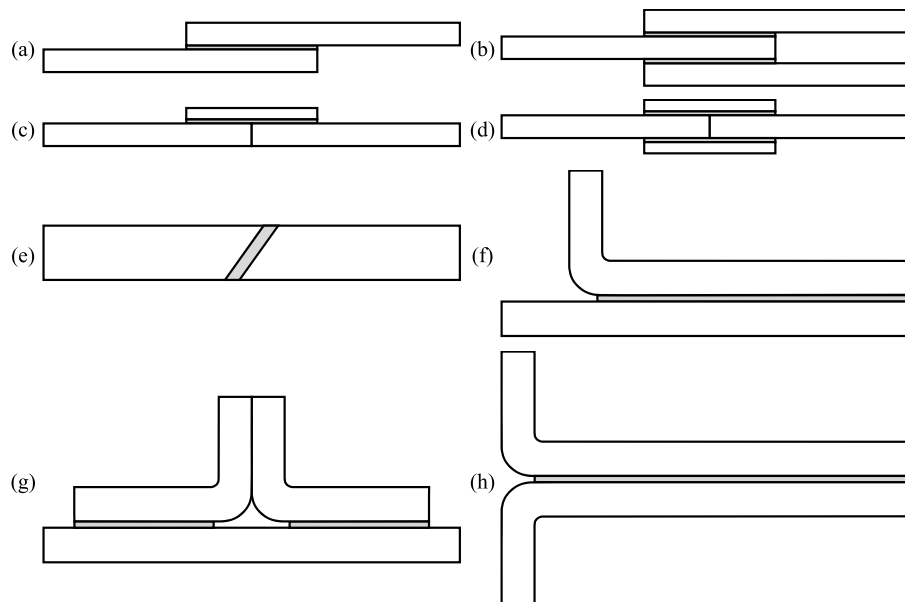

Fig. 1. Typical geometry of SLJ (a), DLJ (b), SJ (SJ) (c), DSJ (d), ScJ (e), single-L joints (f), T-joints (g) and T-peel joints (h).
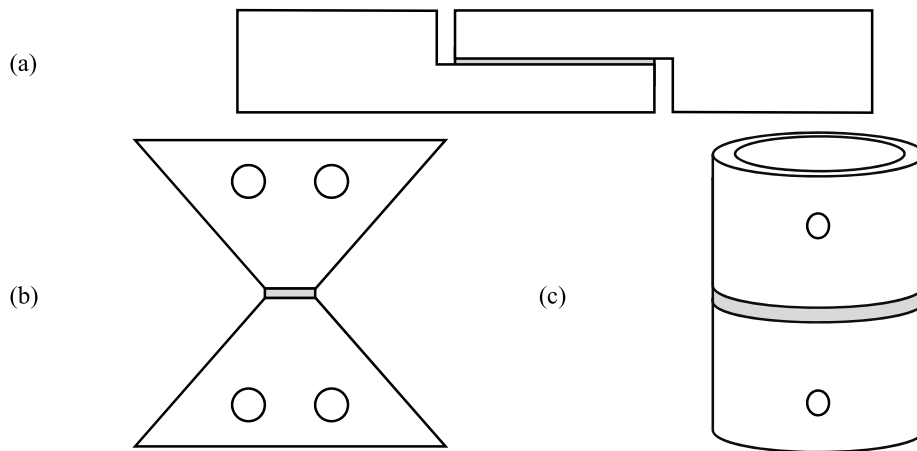
Fig. 2. Typical geometry of the TAST (a), Arcan (b) and Napkin Ring Test (c) specimens.
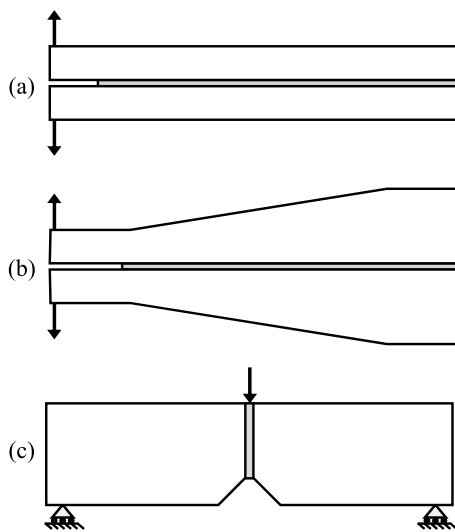

Fig. 3. Typical geometry of the DCB (a), TDCB (b) and SENB (c) specimens.

fracture mechanics, damage mechanics, CZM and the XFEM, being also used to determine tensile cohesive strength (t_n^0), needed for CZM.

The mode II critical strain energy release rate (G_{IIc}) is generally determined with End-Notched Flexure (ENF) [15], four-point ENF (4ENF) [16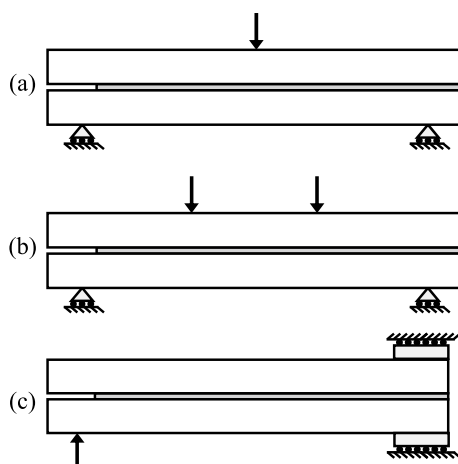] or End-Loaded Split (ELS) [17,18] tests (Fig. 4) but these tests are not standardized for adhesive joints, unlike the tests to determine G_{Ic} [19]. Comparisons between the ENF and 4ENF tests [19] showed that the G_{IIc} predictions from both tests are similar. However, the ENF works better overall because it has more data reduction techniques available, including the Compliance-Based Beam Method that can determine G_{IIc} without needing to experimentally measure crack length evolution, which is difficult in shear tests. These tests are required to perform strength predictions of adhesive joints when using fracture mechanics, damage mechanics, CZM and the XFEM, being also used to determine shear cohesive strength (t_s^0), needed for CZM.

Some tests where the mode-mixity is known can also be performed to obtain the full fracture envelope of the adhesives, which establishes the relationship between G_{Ic} and G_{IIc} for different mode-mixities. Mixed-mode tests include the Single Leg Bending (SLB) [20], the Asymmetrical Tapered Double-Cantilever Beam (ATDCB) [21] and Mixed Mode Bending (MMB) [22], exemplified in Fig. 5. The work of Hasegawa et al. [20] is an example of this, where DCB, TAST with a pre-crack and SLB tests were used to obtain the critical strain energy release rate (G_c) in mode I, mode II and mixed-mode conditions, respectively, which allowed to determine the full fracture envelope for an adhesive. A recently proposed apparatus [21] is able to test adhesive joints under many different mixed-mode ratios, depending on how the loads are applied, which allows the obtention of the full fracture envelope, shown in Fig. 6, with a single device. Mixed-mode ratios with this apparatus can range from pure mode I to almost pure mode II. The most common laws to determine an adhesive fracture envelope are generally the Power law
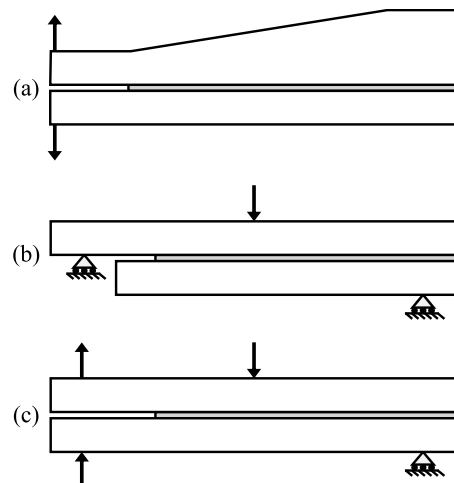

Fig. 4. Typical geometry of the ENF (a), 4ENF (b) and ELS (c) specimens.

Fig. 5. Typical geometry of the ATDCB (a), SLB (b) and MMB (c) specimens.
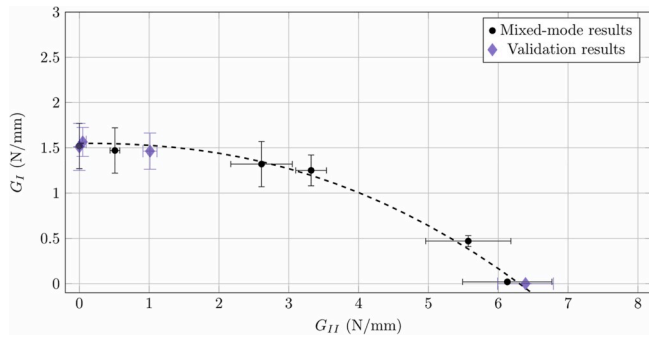
Fig. 6. Example fracture envelope [21].

or the Benzeggagh-Kenane law, which are described in Equations (2.1) and (2.2), respectively:

$$\left(\frac{G_I}{G_{Ic}}\right)^{\alpha} + \left(\frac{G_{II}}{G_{IIc}}\right)^{\alpha} = 1 \tag{2.1}$$

$$G_{Ic} + (G_{IIc} + G_{Ic})\left(\frac{G_s}{G_T}\right)^{\eta} = G_c \tag{2.2}$$

where G_I, G_{II} and G_{III} are the mode I, II and III strain energy release rates, respectively, $G_s = G_{II} + G_{III}$ and $G_T = G_I + G_s$. η and α are material parameters, determined with tests with various mode mixities, which define the fracture envelope.

3. Stress analysis and strength prediction

3.1. Analytical methods

Several analytical methods were developed over the years to predict the strength of adhesive joints. Although these methods still serve a purpose nowadays, as an initial indicator of the joint strength, they have been largely substituted be numerical methods, discussed in detail in Section 3.2, in more complex analyses, or in analyses that need higher accuracy. These methods generally provide the stresses and/or strains in the adhesive layer, which are then used to determine failure by comparing them to adhesive properties.

An extensive review of the analytical methods used to predict the strength of SLJ was made by da Silva et al. [23] in 2009 and a comparison between those different analytical methods was presented in the second part of that paper [24]. This two-part work compares some of the pioneer works in the field, such as the Volkersen's model [25] or the Goland-Reissner model [26], and later models developed before 2009. As the scope of the present review is the current decade, for more details about these older models the work of da Silva et al. [23,24] or the book by Campilho [27] can be consulted, as well as the software of Dragoni et al. [28], which is capable of determining the strength of different types of adhesive joints by using analytical models. Goglio et al. [54] used a structural sandwich model to determine the strength of SLJ and T-peel joints comparing different failure criteria. Recently proposed analytical models to determine the stress distributions in adhesive joints include references [29–34].

Sousa et al. [35] compared different classic SLJ analytical solutions. Their strength predictions showed that the Hart-Smith plastic model [36] is able to correctly determine the joint strength increase with the overlap length (L_O), when brittle or moderately ductile adhesives are used, being more accurate for brittle adhesives (Fig. 7). For very ductile adhesives, the global yielding failure criterion [37] was the only criterion capable of correctly predicting joint strength for different L_O, when compared to experiments. Moradi et al. [38] used FFM, discussed in Section 3.2.2, together with and asymptotic model, to predict the failure strength of SLJ and DLJ. This approach was able to predict the strength
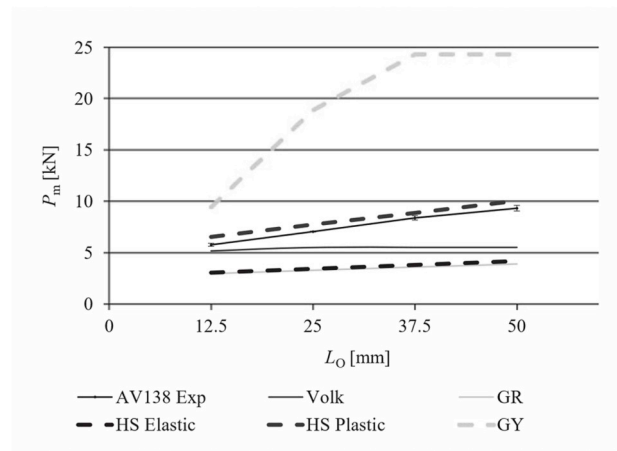

Fig. 7. Strength prediction of a SLJ with a brittle adhesive using different analytical methods [35] (Exp = Experimental; Volk = Volkersen; GR = Goland & Reissner; HS = Hart-Smith; GY = Global Yielding).

decrease with increasing adhesive thickness (t_A). FFM were also used by Weißgraeber and Becker [39] to determine adhesive failure with the stress distribution described by the Ojalvo–Eidinoff model [40]. This approach was able to correctly predict the strength of SLJ with different adhesives, L_O and t_A, when compared to experimental results. The general sandwich-type model of reference [30] was used by Stein et al. [41], together with FFM, to determine the strength of different joints: SLJ, DLJ and T-peel joints. The strength predictions were generally similar to the experimental strength, regardless of L_O, t_A, adherend thickness (t_P) or joint type.

Joints bonded with functionally graded adhesives are a recent research focus, due to their potential to increase joint strength by decreasing the stress concentration at the overlap ends of SLJ, resulting in more uniform stress distributions. Stein et al. [42] compared the stress along the overlap of SLJ with functionally graded adhesives obtained using previous analytical methods [43–45] and a new Improved Shear-Lag Model. This comparison is shown in Fig. 8, for a symmetric adhesive grading, where the GM is the sandwich-type model of reference [45]. The sandwich-type model and the model proposed in Ref. [44], based on the Goland-Reissner model, provided stress distributions very similar to the stress distributions achieved by a Finite Element Method (FEM) model, for different adhesive grading configurations. However, the sandwich-type model is able to predict the stress of different joints, such as DLJ and single-L joints, additionally to SLJ, as it was shown in Ref. [45], while the model of reference [44] is only applicable to SLJ. Even if the shear stress obtained with the model developed by Carbas et al. [43], based on the Volkersen model, predicts a stress distribution different from the FEM, in Ref. [46] it was used to predict the strength of a functionally graded SLJ with good accuracy, confirmed with
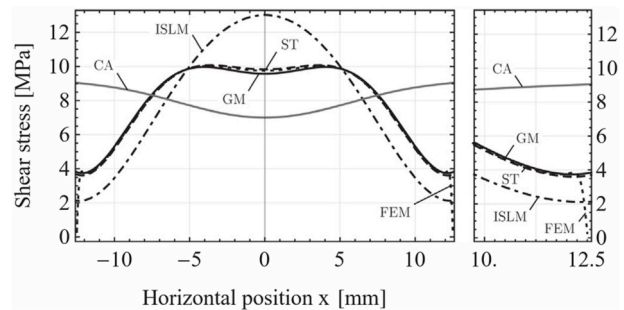

Fig. 8. Comparison between the stress of SLJs with graded adhesives achieved with different analytical models [42] (CA = Carbas' model; ST = Stein's model; GM = General Model).

experiments.

3.2. Numerical methods

The use of analytical methods to solve adhesive joint problems becomes difficult or impossible with the increased complexity of the joints, so it is necessary to use numerical methods, such as the FEM, to properly predict the behaviour of adhesive joints. There are many different numerical methods to evaluate adhesive joints, but the most commonly used method is the FEM [27]. However, advanced numerical techniques, like meshless methods, can also be used to determine the strength of adhesive joints, but their use is currently rare. When evaluating the failure of adhesive joints with the FEM, there are several approaches that can be taken, namely continuum mechanics, fracture mechanics, damage mechanics, CZM or the XFEM. Alternatively, meshless methods can also be used. In this section, when a strength prediction is deemed accurate or good, it is in comparison to experimental results unless stated otherwise.

3.2.1. Continuum mechanics

Continuum mechanics criteria are generally used, together with a FEM analysis, to study the stresses along the mid thickness of the adhesive layer and perform strength prediction [10]. There are several papers, focused on CZM, that perform a separate FEM model with continuum elements in the adhesive layer to visualize the stress variation along its mid thickness line. Some examples are given in Refs. [47,48], discussed in detail in section 3.2.4. Using continuum elements to perform strength predictions is less common nowadays, because the stress singularities at the interface corners lead to increasing stress in that area with increasing mesh refinement. However, there are several recent publications using continuum elements to perform strength predictions of adhesive joints, examples of which include references [49–53]. Traditional failure criteria, such as determining failure using the maximum stress or strain in the middle of the adhesive, are not commonly used nowadays. However, most papers covered in this section use more recently developed criteria. The review of He [2] and the chapter 5 of the book [27] present some older literature covering those criteria. Recently, new failure criteria for adhesive joints have been proposed to attempt to solve some of the problems associated with using continuum mechanics to determine joint strength.

In 2015, Ayatollahi and Akhavan-Safar [55] proposed a new criterion based on the longitudinal strains and the theory of critical distances [56], called Critical Longitudinal Strain (CLS) criterion. This criterion requires at least two experimental tests of SLJ with different L_O to determine its two critical parameters. An example of their determination is shown in Fig. 9. Mesh independency was observed for this criterion and it worked well on SLJ with three different brittle adhesives and geometries. The CLS criterion was later applied to SLJ with varying t_A [57]. The critical parameters determined using a specific t_A could be used for other t_A. It was found that the CLS results are similar to experimental results in most cases, showing a decrease in strength with t_A increases, but when the ratio between L_O and t_A is low the strength prediction is not accurate. Khoramishad et al. [58] tested experimentally SLJ with aluminium adherends of varying t_P. They showed that the critical distance did not change with t_P, while the CLS decreased with t_P, but not linearly. Actually, the decrease starts to get smaller as t_P increases. Their predictions using the CLS criterion were very accurate regardless of t_P or L_O. Recently, the CLS criterion was tested in a plethora of joints, with different adhesives, adherends and L_O [59] to verify its dependency on these parameters. In this work, it was shown that this criterion is not usable when there is adherend yielding. When the adhesive is not very brittle or very ductile, its CLS can be determined using a linear formula. Then, the critical distance can be obtained from just one experimental test. In this work the predictions were also shown to be accurate for the different SLJ. Razavi et al. [60] recently proposed the Critical Normal Strain (CNS) criterion. This criterion uses a critical
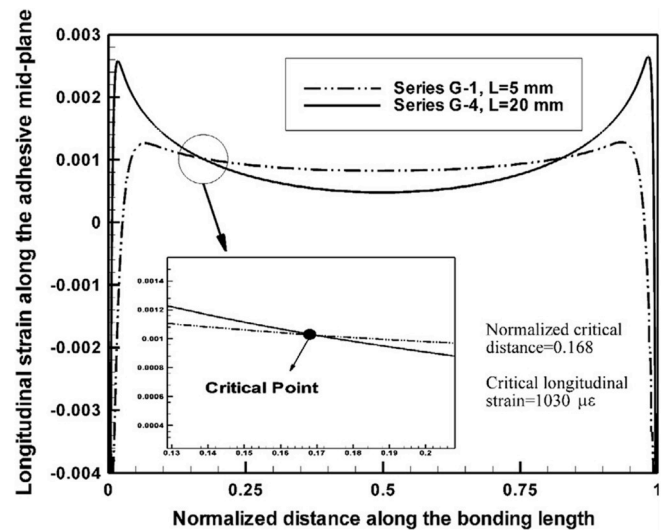

Fig. 9. Determination of the critical distance and the critical longitudinal strain [55].

normal strain at a critical distance to determine joint strength, similarly to the CLS criterion, but using normal strain instead of longitudinal strain. The criterion was shown to be mesh independent and it gave accurate strength predictions for the DSJ to which it was applied.

Karachalios et al. performed a two part study, which experimentally and numerically tested SLJ made of high strength steel [61] and ductile steels [62], bonded with four different adhesives. Their proposed method of joint strength determination for the high strength steel, based on the strain fields provided by a continuum FEM analysis, showed to be accurate for ductile adhesives, but inaccurate when the adhesive is brittle. When the joints are made of very ductile steels, the use of the load at which the adherends started to yield as the limiting factor provided good strength predictions, but not when the steel was only moderately ductile. The same authors also used their strain based criterion to predict the strength of SLJ under bending [63]. Their predictions were close to the experimental strength of the joints for smaller t_P, but when t_P is high the criterion under predicted joint strength. In 2011, Zhao et al. presented a two part study [64,65] analysing the effects of rounding the adherends corners in filleted SLJ, exemplified in Fig. 10, with different radiuses and two different adhesives, one brittle and the other ductile. They showed that rounding the adherend corner removes the singularity in that region. However, the singularity at the edges of the fillet does not disappear. To perform the strength prediction, two new failure criteria were proposed. One of these criteria, for brittle adhesives, takes a weighted average of the stresses over a distance from the adherend corner into account. This criterion proved to be mesh independent and gave acceptable results for the sharp corner. The other criterion, Average Plastic Energy Density Criterion, was introduced for ductile adhesives, and it takes an average of the plastic energy density along a distance from the adherend corner. This criterion proved to be mesh independent and accurate for sharp corners. Overall, joints with
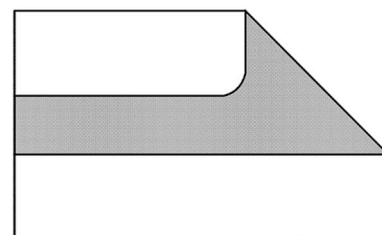

Fig. 10. Example of a rounded adherend corner [64].

the brittle adhesive increased their strength with corner rounding, but the inverse happened when the ductile adhesive was used.

Reis et al. [66] assessed the influence of the adherend's mechanical properties on the strength of SLJ, as well as having different top and bottom adherends. They determined joint failure numerically when the principal stress, integrated over a critical region close to the interface, reached maximum. With this criterion they achieved results with a maximum error of 20% for all the different adherend combinations. They also showed that stiffer adherends lead to stronger joints. Campilho et al. [67] studied a reverse-bent SLJ geometry (Fig. 11). It was shown that using a bent geometry resulted in strength increases, especially for joints with brittle adhesives. They used continuum elements to model the adhesive and the adherends. The failure load was calculated using the maximum shear stress and the maximum strain criterion criteria for the brittle and the ductile adhesives, respectively. Their strength predictions with these criteria were acceptable. Wu et al. [68] have recently compared ScJ and stepped-lap joints with gaps of varying length and location in the adhesive layer. They determined cohesive failure using the maximum shear stress criterion or the maximum shear strain criterion, in the mid-thickness plane of the adhesive. The stress criterion was used when the adhesive behaviour was brittle, and the strain criterion was used when it was ductile. It was shown that ScJ are more affected by gaps than stepped-lap joints, and that using a doubler reinforcement can greatly reduce the strength loss caused by the gap.

3.2.2. Fracture mechanics

Fracture mechanics is able to evaluate the stress or strain singularities generated by discontinuities in materials, unlike continuum mechanics [69]. In adhesive joints, these discontinuities are generally re-entrant corners at the adhesive-adherend interface or defects. Traditional fracture mechanics concepts used to determine crack propagation include the Stress Intensity Factor (SIF) and the Strain Energy Release Rate (SERR), which are related. In mixed-mode loading and plane strain conditions the relation is expressed by:

$$G = K_I^2 \frac{1-\nu^2}{E} + K_{II}^2 \frac{1-\nu^2}{E} \qquad (3.1)$$

being K_I and K_{II} the modes I and II SIF, respectively. There are several techniques to determine the SIF or the SERR, including J-integral [70] or the Virtual Crack Closure Technique [71]. In its most simple form, a line integral, the J-integral is defined by the following formula:

$$J = G = \int_\Gamma \left(W n_1 - T_i \frac{\partial u_i}{\partial x} \right) ds \qquad (3.2)$$

being Γ any path beginning at one face of the crack and ending at the other face of the crack, n is the unit vector normal to the path, $T_i = \sigma_{ij} n_j$ and $W = 1/2 \sigma_{ij} \varepsilon_{ij}$. The VCCT allows to determine the SERR by relating the forces at the crack tip F and with the displacements u in the crack node behind it according to the following formula:

$$G = \frac{Fu}{2bd} \qquad (3.3)$$

being b the joint width and d the distance between the crack tip and the crack node behind it.

Chen et al. [72] used the specific strain energy density criterion to determine crack initiation and propagation in SLJ with different
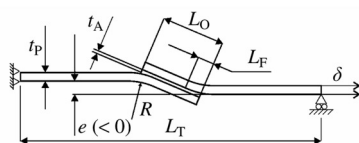
adherends, and adhesives with and without adhesive fillets. The used criterion integrates the strain energy over an element and averages it over the element area, failure is determined by comparing this with the material specific failure energy, determined experimentally. They found that fillets increase joint strength, but they make the joint more sensitive to defects. Their results also showed that joints with brittle adhesives are stronger when the adherends are stiff, while joints with ductile adhesives are stronger when the adherends have a high yield stress. The crack paths and joint strength predicted with this approach were similar to experiments. Afendi et al. [73] determined the strength of ScJ with different adherends, bonded with a brittle adhesive with several t_A. They used corner toughness, which is similar to fracture toughness, to determine failure by evaluating the stress singularity at the adhesive-adherend interface corner. This parameter was shown to be independent from t_A, but it changed with the scarf joint angle. Their results were close to experimental strength for different t_A and scarf angles. Goh et al. [74] compared different solutions to determine the strength of composite ScJ with defects of varying lengths at one of the interfaces and without them. The predictions using the Virtual Crack Closure Technique (VCCT) or Linear Elastic Fracture Mechanics (LEFM), to determine G to compare with G_c, greatly overestimated the strength of ScJ with small defects. However, the VCCT gave very accurate predictions for bigger defects, while LEFM underestimated joint strength in that situation, compared to experimental strength. Comparing to CZM, discussed in Section 3.2.4, the results were good for bigger defects, but CZM were able to determine the joint strength accurately for small defects and crack initiation when no defect was present. Recently, Cameselle-Molares et al. [75] used the VCCT to predict the strength of Fibre Reinforced Polymer (FRP) DLJ. The strength predictions obtained showed good agreement with experimental results. However, this model assumes no plastic deformation, so it is only valid for brittle adhesives. Akhavan-Safar et al. [76] used the maximum tangential stress criterion, with the help of the critical distances concept [56], to determine the strength of SLJ with a pre-crack. Their predictions agreed with experimental results.

The coupled stress-energy criterion, now named Finite Fracture Mechanics (FFM), introduced by Leguillon [77], was used in several recent research works [78–84]. A review of the applications of this method, including adhesive joints, is also found in Ref. [85]. This criterion is able to determine crack initiation and it does not require an initial crack. To initiate a crack, an energetic criterion and a stress criterion must be satisfied, as exemplified in Fig. 12. The energetic criterion provides a lower bound for crack initiation, while the stress criterion provides an upper bound. This criterion is only applicable when brittle adhesives are used. For SLJ bonded with brittle adhesives, this criterion was able to successfully assess the influence of L_O and t_A on joint strength [79,80], finding that joint strength increased with decreases in t_A and increases in L_O. FFM were also able to predict the strength of DLJ and butt-joints with acceptable accuracy, compared to experiments, in a separate work [78]. In 2015, FFM were used to determine the correlation between adhesive stiffness, adherend stiffness, t_P and joint strength for SLJ [86]. It predicted that increasing the adhesive stiffness did not
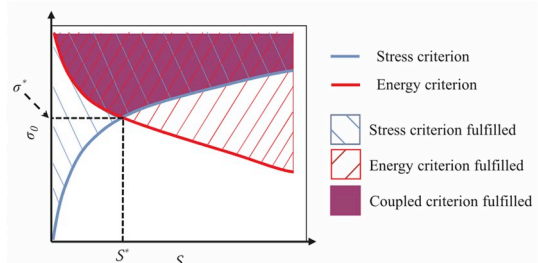
Fig. 11. Reverse-bent SLJ [67].

Fig. 12. Example of the coupled criterion as a function of crack area and imposed loading [83].

increase the joint strength significantly but increasing adherend stiffness and t_P resulted in a noticeable joint strength increase. The effect of adherend length was also studied, maintaining a constant L_O, showing that increasing it results in a strength decrease, reaching a constant value for bigger L_O.

FFM were recently expanded to Three-Dimensional (3D) adhesive joints, being first studied in butt-joints under bending [82] and later in ScJ under tension and bending [83]. In the 3D case, the crack area is determined with the aid of the stress contours at the plane where fracture is expected to occur. The tests performed showed accurate results. Recently, Le Pavic et al. [84] used FFM to determine the strength of a double notched bonded structure, meaning that it had an initial crack. Their predicted strength was very similar to the experimentally determined strength, when using the FEM with FFM, but the strength was underestimated when an analytical method was used with the couple criterion.

3.2.3. Damage mechanics

The Damage Mechanics approach is able to simulate progressive material degradation in the adhesive, meaning that the adhesive progressively loses its stiffness until it reaches a failure point, where it loses all its stiffness. This approach is able to determine arbitrary crack paths unlike CZM, where the crack path is predetermined by the cohesive elements.

García et al. [87] used a Continuum Damage Model (CDM) to determine crack initiation and propagation in a joint used in wind turbines, bonded with a ductile and tough adhesive. Their model used the Drucker-Prager exponential criterion to describe the adhesive elasto-plastic behaviour and the softening was described as linear. They were able to correctly determine the crack path (Fig. 13), as well as the joint strength when compared to experimental tests. Chousal and de Moura [88] proposed a damage model with continuum elements having a triangular traction separation law, meaning that the stress increases linearly until damage initiates, and it decreases linearly, until complete failure. They tested their model in DCB and ENF specimens, being able to predict crack paths and the Fracture Process Zone (FPZ) correctly. Stapleton et al. [89] proposed a FEM formulation with adaptative shape functions and mesh, as an improvement of reference [90]. The shape functions of this method are derived from analytically solving the governing equations of the problem. This method required very few elements and was computationally quicker than a CZM of the same problem. Its strength predictions were also very similar to the CZM predictions for a SLJ and a DCB. Joint failure was determined using a progressive damage model, similar to the CZM. FFM, referred in Section 3.2.2, were also used in a damage model in Ref. [81], where the damage evolution was defined with a triangular law. The strength predictions with this approach were, in general, better that the predictions achieved with the fracture model.

Belnoue et al. [91,92] proposed a new damage model in a two part study. The model uses the Drucker-Prager criterion to model plasticity and a linear softening to model damage. In part I [91], the model was shown to capture the FPZ variation with t_A, caused by the adherends constraining the adhesive. The model was calibrated with ENF tests with different $t_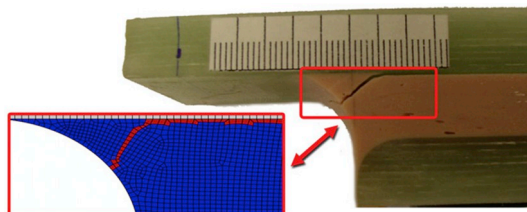A$. Using the critical energy obtained with those tests, the strength predictions of DCB with different t_A were accurate. In part II [92], the proposed damage model was used in DLJ with composite and metal adherends, combined with cohesive elements at the composite-adhesive interface. The strength predictions achieved with this approach were accurate, and it was able to predict adhesive and cohesive failure at the same time. This model was also able to correctly assess the influence, on joint strength, of t_A and of a compressive load applied at the overlap.

Sugiman and Ahmad [93] have performed a comparison between CZM, more common in the study of adhesive joints, and a CDM with linear softening. The use of CZM resulted in marginally more accurate strength predictions, but CZM are not able to determine the crack path, which the CDM accurately predicted. In this work, it was also demonstrated that the adhesive elements should have an aspect ratio of 1. Riccio et al. [94] assessed the applicability of a damage model with a linear softening phase, in ScJ and in joints under three-point bending. Their strength predictions were similar to the experimental strength of the joints. Furthermore, their model was also able to determine crack paths and damage location correctly in both examples. Zhang et al. [95] used a CDM with linear softening to predict the strength of composite-metal ScJ. Their predictions were shown to be accurate when compared to experimental results. Using this knowledge, they compared the effect on joint strength of using different metals and composite stacking sequences. Kim and Hong [96] proposed a mixed-mode damage model, with a traction-separation law having an exponential hardening section, capable of correctly capturing the ductility of different adhesives, and an exponential softening section, with a different formula defining it. The Benzeggagh-Kenane criterion was used to determine damage propagation and a second order criterion was used to determine damage initiation. The model was used in SLJ with different t_A and t_P, and with and without adhesive fillets. It was shown that joint strength increased with fillets and t_P. Regarding t_A, while the joint strength decreased with this parameter when there are no fillets, in the presence of fillets the joint strength increases with t_A. The comparisons with experimental results were also good.

3.2.4. Cohesive zone models

The use of CZM to study damage and crack propagation in adhesive joints has been widely studied in recent years. This method is generally used with the FEM, having special paired nodes that behave accordingly to an established cohesive law, i.e. traction separation law [27]. Cohesive elements have a stress criterion that defines damage initiation and a fracture criterion that defines crack propagation. Besides the works discussed in more detail in this section, several other academic works have also used CZM to predict the strength of adhesive joints, such as [74,92,93,96–105]. CZM first appeared in the late 1950s/early 1960s in the works of Barenblatt [106] to study cracks in brittle materials and Dugdale [107] to study yielding in steel sheets containing cracks. One advantage that CZM have over other approaches is that their strength prediction is mesh independent, as shown in Fig. 14 and proven by

Fig. 13. Comparison between the experimental crack path and the predicted crack path with a damage model [87].
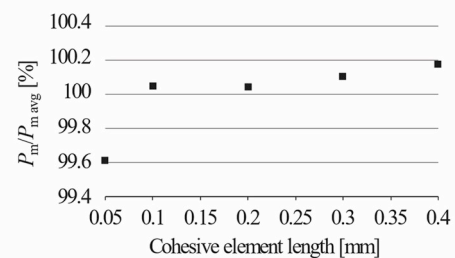

Fig. 14. Mesh dependency of CZM [111] (P_m = maximum load; P_{mavg} = average maximum load between the different discretizations).

several mesh dependency studies [108–110]. This is due to the damage growth being defined by an energetic criterion averaged over an area, instead of taking values from a single point.

There are two main different approaches to CZM, the local approach and the continuum approach. Concerning adhesive joints, the local approach uses cohesive elements to connect superimposed nodes of elements, thus representing a zero-thickness interface. In the continuum approach, cohesive elements simulate the whole adhesive bond, which has a finite thickness, connecting the two adherends. The differences between these two approaches are illustrated in Fig. 15. In the local approach the cohesive elements only simulate damage growth between the elements connected by them, and the plastic properties of the adhesive are simulated by solid finite elements; while in the continuum approach the stiffness of the CZM elements represents the adhesive layer stiffness in each mode of loading. The continuum approach has been the focus of more intense study. Thus, most papers referred in this section adopt that approach, and the ones that do not explicitly mention that they adopt the local approach.

O'Mahoney et al. [112] performed a Taguchi analysis of composite SLJ using the local approach, having zero thickness cohesive elements in the adherend/adhesive interface, and continuum damage elements in the adhesive. With this analysis they found that adhesive strength, interface fracture toughness and adhesive ductility have the most significant impact in the strength of SLJ. Sugiman et al. [113] investigated the influence of using zero thickness cohesive elements at the middle of the adhesive layer or at the adhesive/adherend interface, with the other adhesive elements modelled as continuum elements. They found that cohesive elements in the middle gave slightly more accurate results for SLJ, compared to cohesive elements in the adhesive/adherend interface. More recently, Heshmati et al. [114] used the local approach to predict the strength of DSJ, with good agreement with the experimental tests. They also showed that using the symmetry of the DSJ to make the numerical model resulted in strength over predictions. Geleta et al. [115] have employed an approach different from the local and continuum approaches by discretizing the adhesive layer with continuum elements and then inserting cohesive elements between every one of them. They tested this approach in inclined adhesive joints, and the strength predictions with this model showed good agreement with experimental results. An advantage of this approach, when compared to conventional CZM approaches, is that it does not restrict the crack to a predefined path, as shown in Fig. 16. Generally, an implicit formulation is used in CZM static applications, but some authors have used explicit formulations [116,117] with accurate strength predictions for SLJ with composite adherends, being also able to take into account delamination with cohesive elements in the adherends.

The cohesive law can take many different shapes, including triangular, linear-parabolic, polynomial, exponential and trapezoidal [69]. The most simple and commonly used shape is the triangular shape [27].
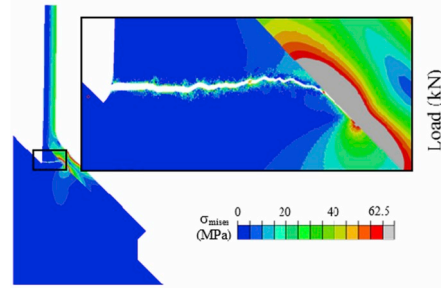

Fig. 16. Crack path achieved with the approach proposed by Geleta et al. [115].

This shape gives very good results when dealing with brittle adhesives, and it can also give acceptable results for ductile adhesives under certain conditions, with minor strength under predictions [118–121], but it was also shown that they can lead to non-negligible strength under predictions of very ductile adhesives [122]. Due to being implemented in ABAQUS® and its simplicity, the triangular law is the most commonly used law. Therefore, unless stated otherwise, it is the law used in the works cited in this section. The differences between some of the different cohesive law shapes can be seen in Fig. 17, where the parameters defining the cohesive law: critical strain energy release rate (G_c), cohesive strength (t^0), displacement at peak traction (δ^0) and softening initiation displacement (δ^s), are the same for all shapes.

Fernandes and Campilho [123] studied DCB specimens, to ascertain the influence of the cohesive law shape and parameters in the strength prediction of joints under pure mode I traction. They found that, in this case, triangular and trapezoidal law shapes provide similar, and accurate, strength predictions for brittle and ductile adhesives. Regarding the impact of the parameters, it was shown that G_{Ic} impacts more significantly the strength of the joint than the t_n^0 for all tested adhesives. With a similar purpose in mind, but for mode II loading instead of mode I, the same authors have later studied ENF specimens [124]. They found that, in this case, the triangular law was more suitable for brittle adhesives, while its accuracy decreased with the increase of adhesive ductility, where the trapezoidal law was more accurate. G_{IIc} variations were the most impactful on the strength prediction of brittle adhesives, while t_s^0 variations were the most impactful on the strength prediction of ductile adhesives. Campilho et al. [118] compared the strength prediction of SLJ with varying L_O using different cohesive law shapes. Triangular laws were more adequate for brittle adhesives, while trapezoidal laws were more adequate for ductile adhesives. Even so, the difference in strength prediction between triangular and trapezoidal laws for ductile adhesives was smaller than 10%, so it might be preferable to use the triangular law in this case, due to its simplicity. More recently, a comparison between
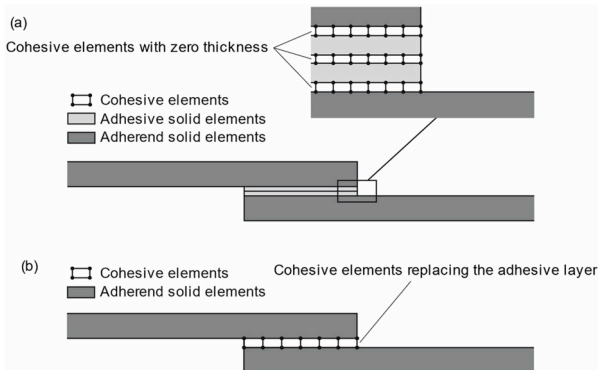

Fig. 15. Cohesive elements with the local approach (a) and with the continuum approach (b) in an adhesive joint.
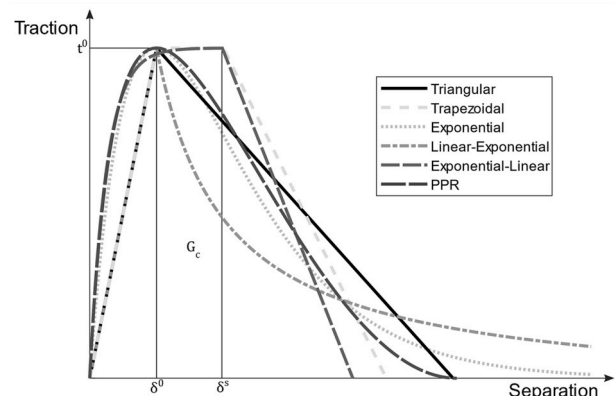

Fig. 17. Comparison of the different traction separation laws.

different cohesive law shapes, using three different adhesives, was also performed by Carvalho and Campilho in SLJ [119] and DLJ [125], with findings similar to Ref. [118]. For $L_O \leq 50\,mm$, the difference between the various cohesive law shapes was very small. Therefore, using an inadequate cohesive law shape was not overly harmful in these cases. Zhang et al. [126] investigated different cohesive law shapes on DCB and butt-joints, with brittle and ductile adhesives. They found that the law shape has a big influence on the strength prediction of butt-joints and a smaller, but not negligible, influence for DCB. The triangular law gave the most accurate predictions for both joints with the brittle adhesive, while for the ductile adhesive the exponential law is the most suitable when dealing with butt-joints and the trapezoidal is the most suitable when dealing with DCB.

In recent years, some authors have proposed more complex cohesive law shapes to better define the properties of adhesive bonds. An example of that is the Park-Paulino-Roesler (PPR) law [127]. This law has a parameter that controls the curvature of the softening part of the law, making it adaptable for different adhesive types. It has been successfully applied to adhesive joints such as DLJ [114] and T-peel joints [128,129]. In 2012, Anyfantis and Tsouvalis [47] also introduced a new CZM law shape, an exponential-linear law, initially exponential and with linear softening when damage initiates. In this initial study, they applied this law to a ductile adhesive in a SLJ and a DSJ. This study showed that the proposed law could predict the strength of both joints with high accuracy and a smaller error than the trapezoidal or the PPR laws. Furthermore, the overall load-displacement curves proved to be much closer to the experimental load-displacement curves that the other laws. This law shape was later also applied to ductile adhesives in metal-composite DLJ [130] and SLJ [131], and 3D SLJ, DLJ [132,133], ENF and DSJ [120], with varying degrees of success, generally providing load-displacement curves with a shape very similar to the experimental one, but in some cases over predicting the joint strength. Due to the need to determine the correct law shape for different problems, Xu et al. [134] proposed an Interpolation-Based CZM (ICZM) that can model the arbitrary shape of an adhesive's traction-separation law with high accuracy. Their approach is easier to understand and implement than the approach of Shen and Paulino [135], and the strength prediction using an ICZM law shape compared favourably with experimental results for a DCB specimen under pure mode I traction.

An important geometrical parameter when considering adhesive joints' design is t_A. When using CZM, the effects of t_A on the joint strength are generally considered by modifying the cohesive law parameters. Some authors have performed experimental tests to assess the effects of t_A on the cohesive law parameters. Through a DCB test, Ji et al. [136] showed that t_A affects the mode I fracture parameters of the adhesive layer t_n^0 and G_{Ic}. Actually, G_{Ic} increases with t_A, while t_n^0 decreases, as shown in Fig. 18a. The G_{Ic} increase with t_A was also verified in the experimental works of references [11,12,137]. Ji et al. [15], performing

ENF tests, verified that t_s^0 and G_{IIc} both increase with t_A, as shown in Fig. 18b. The same G_{IIc} increase was also observed by Marzi et al. [12]. However, da Silva et al. [138] showed that G_{IIc} does not increase with t_A when the adhesive is brittle. Carlberger et al. [137] found that G_{IIc} increases with t_A below 0.2 mm, but afterwards it remains relatively constant. With DCB and ENF tests, Boutar et al. [139] found an increase of G_{Ic} and G_{IIc}, respectively, with t_A, until this variable became much bigger than the FPZ radius of the fracture process zone. After a certain point, G_{Ic} and G_{IIc} decreased. Ji et al. [140] also performed a SLB test to assess how t_A affected the fracture parameters under mixed-mode loading. This test showed that G_{Ic}, G_{IIc} and t_s^0 increase with t_A, but t_n^0 decreases, as in the pure mode I and mode II tests.

The tests with varying t_A thus show that the fracture parameters of an adhesive layer are highly dependent on this parameter. The changes in the fracture properties caused by increasing t_A are also different from adhesive to adhesive, but G_{Ic} and G_{IIc} generally increase with t_A if the adhesive is sufficiently ductile. However, this increase is limited by the allowable plasticization of the adhesive at the crack tip. Some authors also performed CZM predictions, in addition to experimental tests, to verify the t_A effect. For pure mode II fracture, Figueiredo et al. [141] showed that the joint strength increased with t_A, and the cohesive parameters, fracture toughness and separation strength, generally increased with t_A as well. The strength predictions of this work with two different t_A are shown in Fig. 19. Liao et al. [142] investigated the effects of t_A and angle of ScJ, showing that lower angles and t_A lead to bigger maximum loads, but lower maximum displacements. Their numerical predictions also showed a good agreement to experimental results of previous works. Xu and Wei [143] simulated SLJ with different t_A with success, demonstrating that lower t_A leads to a bigger joint strength. Their numerical results agreed well with experimental results for the brittle adhesive, but the strength of the ductile adhesive was under predicted for the smallest t_A. Demiral and Kadioglu [144] also demonstrated, with a CZM, that SLJ strength decreases with t_A, but very slightly when compared to the strength increase caused by increasing L_O.

Martiny et al. [145,146] continued the approach originally used by Pardoen et al. [147] which uses a local CZM approach, with cohesive elements near one adhesive/adherend interface or in the middle of the bondline depending on where the crack occurred experimentally, separating the adhesive fracture energy into two components. The intrinsic work of fracture (Γ_0) associated with the damage and fracture of the cohesive zone and the energy expended in the bulk of the adhesive (Γ_b). Γ_0 is not influenced by the geometry of the adhesive joints and it is considered to be a material property. Γ_b is dependent on the adhesive geometric parameters, such as t_A and t_P, they showed that tough adhesives result in almost constant Γ_b, while for ductile adhesives Γ_b tends to increase with t_A until a certain point where it starts to decrease. When t_A gets much larger than the plastic dissipation zone, they found that Γ_b
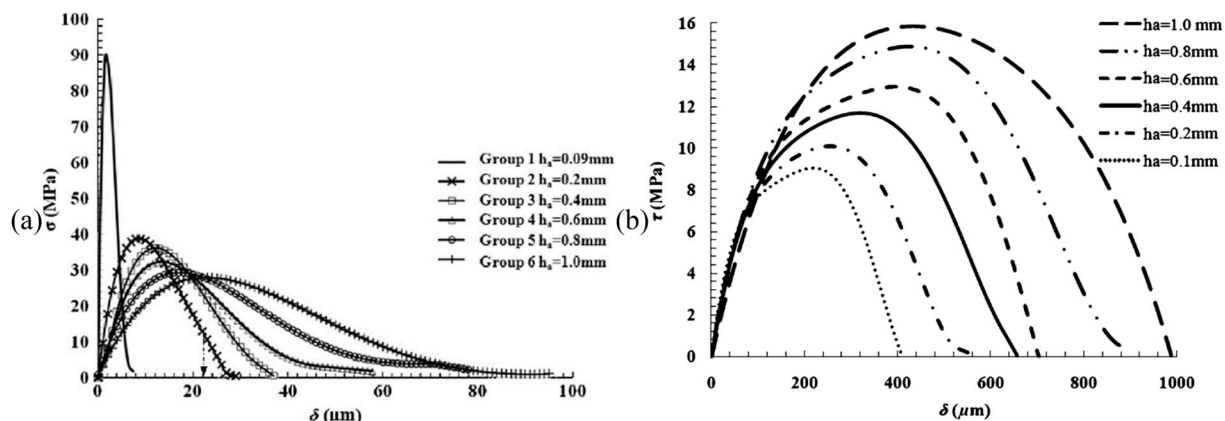

Fig. 18. Change in the experimental obtained traction (σ) [136] (a) and shear (τ) cohesive laws [15] (b) with adhesive thickness: ha −.t_A
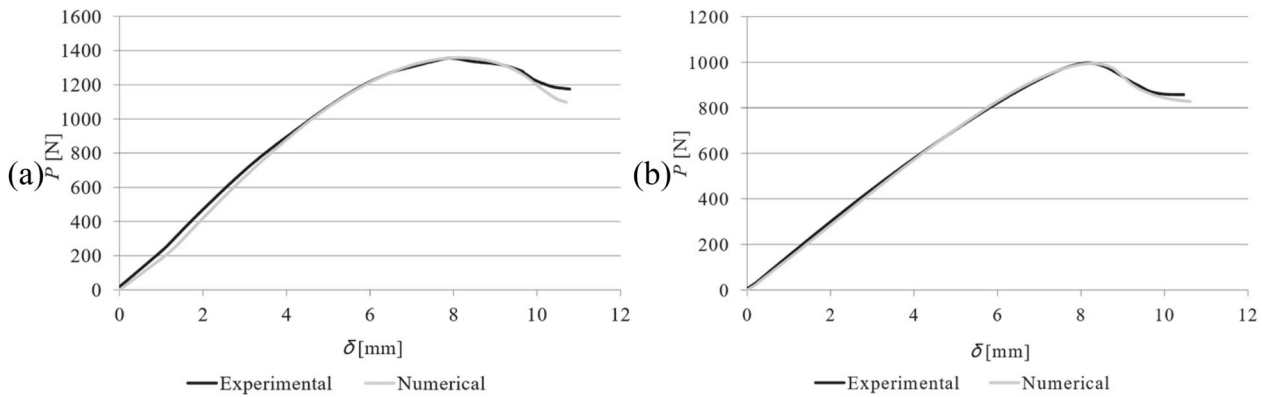
Fig. 19. Strength prediction with $t_A = 0.2$ mm (a) and $t_A = 2$ mm (b) [141].

tends to a constant value, because the constraining effects of the stiffer adherents are not felt.

Other authors focused on the influence on the CZM parameters on the strength predictions. Teixeira et al. [14] demonstrated that, for pure mode I loading by DCB and TDCB specimens, using higher t_n^0 had a minor impact on the joint strength regardless of the specimen. On the other hand, a lower t_n^0 resulted in a non-negligible strength decrease for DCB and a minor strength decrease for TDCB. A higher or lower G_{Ic} resulted in more noticeable strength increases or decreases, respectively, showing it is important to use a correct G_{Ic} in CZM. Azevedo et al. [148] showed that, for pure mode II loading by the ENF test, using a much lower t_s^0 had the biggest effect on joint strength, reducing it, regardless of the adhesive ductility. Changing G_{IIc} resulted in changes to the joint strength, but it did not change the stiffness of the load-displacement curve, while changing t_s^0 does. Ridha et al. [149] performed numerical and experimental tests to assess the strength of bonded scarf repairs, where the numerical tests proved to be accurate. They then performed several numerical simulations to verify he influence of the CZM parameters and law shapes. Their results show that trapezoidal and triangular laws are very sensitive to decreases in t^0 and G_c, and less sensitive to increases; while exponential laws are relatively insensitive to changes in t^0, and very sensitive to any changes in G_c. Campilho et al. [150] studied the effects of the CZM parameters on SLJ, using a triangular cohesive law shape. Smaller G_c values input in the SLJ numerical models to simulate the adhesive generally resulted in a significant joint strength decrease, while higher G_c caused only in a minor increase of joint strength. Regarding t_n^0, higher values resulted in negligible changes in the joint strength, while lower values resulted in a moderate decrease. Finally, smaller or higher values of t_s^0 resulted in a significant strength decrease or increase, respectively. The changes in maximum load when G_{Ic} and t_n^0 are modified are shown in Fig. 20. Fernández-Cañadas et al.

[151] performed the same study for the same adherends and adhesive, but also using trapezoidal and linear-exponential law shapes. They found that changing the parameters had similar effects, regardless of law shape, and that the trapezoidal law gave the most accurate strength estimation, because of the adhesive's ductility. Recently, Rocha and Campilho [108] have studied how other parameters, namely the tensile (E) and shear (μ) moduli of the adhesive, affect the strength prediction calculations. It was shown that changing E or μ of ductile adhesives did not influence the strength predictions by much, while brittle adhesives were only affected when E and μ were severely decreased, which caused a strength increase. Few works also studied the temperature effect on the CZM parameters. By means of DCB and ENF tests, Fernandes et al. [152] demonstrated that temperature has an effect on cohesive law parameters and, consequentially, on the joint strength. The tested adhesive showed a strength decrease for temperatures of 50 °C when compared to 0 °C and 25 °C.

The mixed-mode criterion in CZM modelling is also highly relevant for the outcome of the simulations, and few researchers addressed this issue. In 2017, Santos and Campilho [153], performed experimental tests and CZM simulations of DCB, ENF and SLB specimens with composite adherends, to determine the fracture envelope of three adhesives: Araldite® AV138, Araldite® 2015 and Sikaforce® 7752. They found that a power law exponent of $\alpha = 1/2$ works best for the Araldite® AV138 and Araldite® 2015, while $\alpha = 2$ was suited for the Sikaforce® 7752. Nunes and Campilho [154] performed the same kind of study, but using TDCB, ENF and ATDCB specimens, and steel adherends instead of composite adherends. The same crack growth parameters were determined for the three adhesives, showing that the determination of this parameter is independent of the test performed and adherends used. Sadeghi et al. [22] also developed a fracture envelope for the adhesive Araldite® 2015, using DCB and MMB specimens and a B–K law, instead of the power law. They found a characteristic parameter $\eta = 2.19$ for this
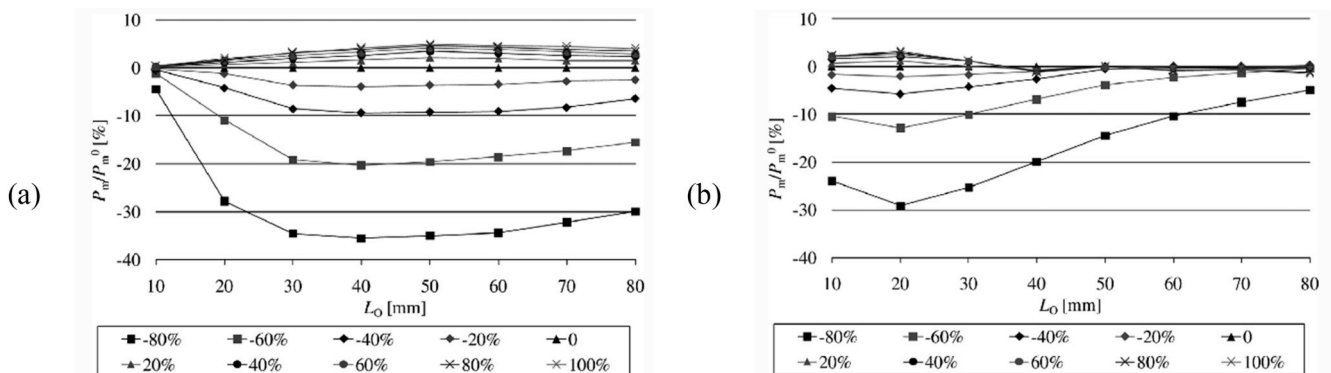

Fig. 20. Variation of the maximum load with L_O and changes in G_{Ic} (a) t_n^0 (b) [150] (P_m^0 – maximum load with the initial parameters).

adhesive. Their numerical strength predictions using this B–K law and a local approach showed good agreement with the experimental results. In Ref. [21], the experimentally obtained α with a developed mixed-mode apparatus was applied to a CZM model, which provided accurate strength predictions for different mode-mixities.

A large amount of available CZM works addresses the strength prediction of typical adhesive joint geometries. Nunes et al. [155] expanded the work of Fernandes et al. [156] by analysing both SLJ and DLJ with three distinct adhesives. They found that DLJ have around double the strength of SLJ with the same adhesive. The CZM strength predictions were consistent with the experimental observations, except when using a ductile adhesive due to adopting a triangular law shape. Moreira and Campilho [157] analysed adhesive scarf repairs, with aluminium adherends and reinforcements, bonded with a brittle and a ductile adhesive. Their results showed good agreement with experimental tests. They found that the reinforcements increase the strength of the repair significantly and, if they are thicker, this increase is bigger. Li et al. [158] studied scarf joints with composite adherends and showed that using cohesive elements in the adhesive layer and in the interface between composite plies results in high accuracy modelling. It was shown that higher t_P and lower scarf angles lead to a bigger joint strength. CZM were also used in T-peel joints [159] with good accuracy when compared to experimental results. In this work, it was shown that adhesives with higher G_c but lower t^0 result in stronger joints. It was also demonstrated that filling the gap between the curved adherends with adhesive resulted in considerable joint strength increases. Besides the standard joints presented until now, CZM have been successfully used to simulate more complex joints, with real world applications. Examples of this include joints in wind turbine blades [160] or adhesive joints in Glass FRP sandwich panels [161–163]. Using a local approach, Marques et al. [164] analysed a joint with mixed adhesives for aerospace applications. Their numerical results agreed well with the experimental tests and showed that the joint strength, using mixed adhesives, is similar to the joint strength using only a strong but brittle adhesive, in the analysed case.

Due to the accuracy of CZM, when compared to experimental results, several authors have used CZM to assess the influence of different geometric changes to the adhesives or the adherends, examples of which are shown in Fig. 21. Luo et al. [165] showed that the strength of SLJ can be improved by having spew fillets and by increasing t_P, with a good correlation between the experimental results and CZM predictions. Pinto et al. [166] analysed the strength of SLJ with recessed adherends, with different recess configurations. It was found that the recess depth has a bigger influence in joint strength than the recess length. The joint strength increased with increases in recess depth and length. Their numerical results were corroborated by experimental tests. Moya-Sanz et al. [167] studied the effects of various geometric changes to SLJ with a mildly ductile adhesive. They studied different chamfering configurations and angles, as well as different adherend recessing depths and lengths. They found through CZM that recessing the adherends increased the joint strength, but chamfering the adhesives and adherends resulted in a bigger strength increase. Recently, Liu et al. [48] compared standard SLJ with curved SLJ and SLJ with a joggle. Their CZM analysis showed that the joggle slightly reduced the joint strength, and that the joint curvature had a negligible effect on the joint strength, as long as the curvature radius is big, i.e. with less pronounced curvatures. Recently, Ribeiro et al. [168] studied the effects of gaps in the adhesive layer of a SLJ, by performing experimental and CZM tests. They found that brittle adhesives are less effected by gaps than ductile adhesives. The joint strength was accurately predicted when using the brittle adhesive but, using the ductile adhesive, the strength was under

predicted due to using a triangular cohesive law shape. Xu and Wei [169] performed a similar test and compared their CZM results to the experimental results of reference [170]. Their results are close to the experimental results and to the results of Ribeiro et al. [168] with the brittle adhesive. Additionally, they found that changing the location of the gap from the centre to one of the sides has a negligible effect in most cases. However, when the gap is big, moving it towards an overlap edge increases slightly the joint strength. Their simulation of weak bonding showed that joint strength decreases when the weak bonding area increases.

The term "hybrid joint" can be viewed by two ways: material or joining technique hybridization, and both cases were recently extensively studied using CZM. For the first type, in 2018, Banea et al. [171] studied how using different adherends affected the strength of SLJ. They observed that joints with the same adherends support higher loads than joints with different adherends. They also showed that it is preferable to have geometrically balanced adherends ($t_{P1} = t_{P2}$) instead of stiffness balanced adherends ($E_1 t_{P1} = E_2 t_{P2}$), for joints with different adherends. Since the CZM used was triangular, and not trapezoidal, the numerical predictions were slightly lower than the experimental results in most cases, because the adhesive used was ductile. Ribeiro et al. [172] used an approach similar to Ref. [122], with zero thickness cohesive elements in the composite adherend and continuum cohesive elements in the adhesive, to model multi-material SLJ (aluminium + composite). Their results showed a good agreement with the experiments for different L_O and adhesives, despite using a triangular law for a ductile adhesive. Alves et al. [173] assessed the effects of joining different adherends in ScJ of varying angles. Their CZM model was able to predict joint strength with very small errors for two types of adhesives, one brittle and another ductile. They showed that having dissimilar adherends affected more the strength of joints bonded by the brittle adhesive, and lower angles result in stronger joints. It was also demonstrated that joints bonded with the ductile adhesive supported higher loads than joints bonded with the brittle adhesive. Avgoulas and Sutcliffe [174] proposed a joint between Carbon FRP and steel adherends, where the steel adherends were perforated in the joining area to create a stiffness gradient. Their experimental and numerical results showed good agreement, and a significant strength increase with the perforation.

There are also some works focused on hybrid joining techniques that used CZM to predict their strength and eventually compare with standard adhesive joints. Works on weld-bonded SLJ [175] showed that, in some cases, these joints have a minor advantage when compared to adhesive joints, while in others, their strength is roughly the same. In Ref. [176], which used CZM to model the weld-spot and the adhesive, the strength of these joints was predicted with a small over estimation. In Ref. [177] weld-bonded T-peel joints were shown to be stronger that adhesive or spot-welded T-peel joints. In this case, CZM were used to model both the adhesive and the nugget, being able to predict the strength of these joints accurately. Sadowski et al. [178] showed that the use of the hybrid technique can lead to a doubling of the joint strength, when compared to spot welded joints. Their numerical model, with cohesive elements in the adhesive, solid elements in the adherends and a point-to-point connection modelling the welding, proved to accurately predict the strength of weld-bonded joints. In Ref. [179], hybrid bonded/bolted SLJ were tested experimentally and numerically, with a good match. The numerical model had cohesive elements in the adhesive and continuum elements in the adherends and the bolt. The results showed that making the joint hybrid does not necessarily increase its strength, and that the increase in strength is dependent on the on the properties of the materials used.
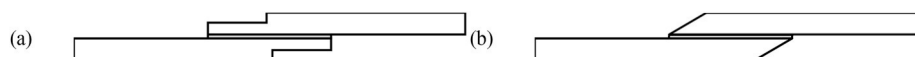

(a)   (b)

Fig. 21. Examples of geometric changes: adherend recessing (a) and adherend chamfering (b).

3.2.5. eXtended finite element method

The XFEM originated in 1999 when Moës et al. [180] developed a method based on the FEM with an enriched displacement field near the crack. This method is based on the partition of unity first presented by Melenk and Babuška [181]. First applied to general fracture mechanics problems, its use in adhesive joints is recent. The main advantage of the XFEM when compared to CZM is their mesh independent crack propagation [97]. The commercial software ABAQUS® has an imbedded XFEM formulation that can predict crack initiation with different criteria. Currently there are six available criteria. In the maximum principal stress (MAXPS) and maximum principal strain (MAXPE) criteria, the crack propagates in the direction perpendicular to the maximum principal stress (σ_{max})/strain (ε_{max}) direction and when the following occurs:

$$1 = \left\{ \frac{\sigma_{max}}{\sigma_{max}^0} \right\} or 1 = \left\{ \frac{\varepsilon_{max}}{\varepsilon_{max}^0} \right\}, \tag{3.1a}$$

where σ_{max}^0 is the allowable maximum principal stress and ε_{max}^0 is the allowable maximum principal strain, both being material properties. In the maximum stress (MAXS) and maximum strain (MAXE) criteria, the crack propagates horizontally or perpendicularly, defined by the user, and initiates when these criteria are met:

$$1 = \max \left\{ \frac{t_n}{t_n^0}, \frac{t_s}{t_s^0} \right\} or 1 = \max \left\{ \frac{\varepsilon_n}{\varepsilon_n^0}, \frac{\varepsilon_s}{\varepsilon_s^0} \right\}, \tag{3.2a}$$

being t_n and t_s the current normal and shear stresses; the strain parameters, ε_n and ε_s, have similar significance. $_s$ and ε_s^0 are the maximum allowable normal and shear strains, respectively. The quadratic stress (QUADS) and quadratic strain (QUADE) criteria also promote horizontal or perpendicular crack propagation, defined by the user, and initiation is defined by:

$$1 = \left\{ \frac{t_n}{t_n^0} \right\}^2 + \left\{ \frac{t_s}{t_s^0} \right\}^2 or 1 = \left\{ \frac{\varepsilon_n}{\varepsilon_n^0} \right\}^2 + \left\{ \frac{\varepsilon_s}{\varepsilon_s^0} \right\}^2. \tag{3.3a}$$

After the adhesive is damaged, according to one of the described criteria, this damage progresses through an element, reducing its ability to carry load progressively, following a material softening law, which relates traction and separation. The discussion of the works in this section always pertains to linear softening laws. Actually, some authors tested the exponential law embedded in ABAQUS®, but it provided very inaccurate strength predictions [182,183].

One of the first works using XFEM in adhesive joints was presented in Ref. [184] where the XFEM formulation of ABAQUS®, using the MAXPS criterion, was used to determine the strength of a DCB specimen with an initial crack. The predicted joint strength matched closely the experimental strength in this simple, pure mode I, loading. Later, Campilho et al. [185] tested the same DCB geometry, but this time under different temperatures. The results showed that the strength of the adhesive, and consequentially of the joint, decreased with increases in temperature, especially if the adhesive glass transition temperature is exceeded, coincident with a severe fracture toughness decrease. Using the MAXPS criterion, the predicted strength for all temperature conditions was similar to the experimental strength. Campilho et al. [111] used the MAXPS and MAXPE criteria to determine the strength of SLJ and DLJ, and compared it with CZM and experimental results. This implementation of XFEM led to crack initiation in the adhesive bond, as expected, but in subsequent steps the crack would propagate into the adherends, which is incorrect. Therefore, the considered formulation was found to be unsuitable to simulate damage propagation, but suitable to simulate damage initiation, for the tested brittle adhesive. However, this approach has shown to be mesh dependent. The XFEM strength prediction was acceptable for different L_O, but below the experimental strength and less accurate than the CZM strength prediction.

More recently, in Ref. [156], the same type of study was performed, but only for SLJ, with three different adhesives, and using the six criteria embedded in ABAQUS®. The predictions were accurate for brittle adhesives but became less accurate as the ductility of the adhesives increased, being completely inaccurate for very ductile adhesives. It was also shown that the results are mesh dependent and a single element along the adhesive layer thickness provided the most accurate results for SLJ. Strain-based criteria were shown to estimate well the joint strength while the stress-based criteria were inaccurate, contrarily to the other works shown in this section, because here the strength was approximated to the crack initiation load, due to difficulties in modelling crack growth. Santos and Campilho [186] used the XFEM to predict the strength of DLJ with three different adhesives, using the six damage initiation criteria embedded in ABAQUS®. The stress-based criteria MAXS and QUADS were the most accurate, with small errors for all adhesives. They also studied the results obtained with different values of α in the power law propagation criterion. The most accurate results were obtained with $\alpha = 1$ for all adhesives. Xará et al. [182] investigated the strength of single-L joints through experimentation and the XFEM. Joints with different t_P for the L adherend were tested, and it was found that the joint strength increases with t_P. A comparison between the different criteria showed that the MAXS and QUADS provided similar, and accurate, strength predictions, while the other criteria either over predicted or under predicted the joint strength. Machado et al. [183] investigated stepped-lap joints with different L_O. Experimental comparisons with SLJ and DLJ showed that stepped-lap joints are generally stronger than SLJ, but weaker than DLJ. The experimental and numerical tests showed that the joint strength increases with L_O, similarly to other types of joints. The most accurate strength predictions were achieved with the MAXS and QUADS criteria, having errors generally smaller than 10%.

Mubashar et al. [97] presented a combined XFEM-CZM approach to model SLJ with fillets, using a triangular CZM at the adhesive-adherend interfaces and the XFEM for the rest of the adhesive, including the fillet, with the MAXPS criterion determining crack propagation in the XFEM elements. This approach provided accurate strength predictions. The crack was predicted to start in the fillet region near the lower adherend corner and propagate towards the upper adherend, continuing near that adhesive-adherend interface, which was also observed experimentally. The predicted crack path is shown in Fig. 22a. Stuparu et al. [98] used a similar modelling approach to predict the strength of SLJ with different t_A and an initial crack. Cohesive elements with a triangular law were used at the adhesive-adherend interfaces, and XFEM for the rest of the adhesive, with the MAXPE criterion determining crack propagation. This model was able to successfully predict the strength decrease for higher t_A. A disadvantage of the XFEM-CZM approach is the crack's inability to propagate away from the cohesive elements once it starts propagating through cohesive elements. Stein et al. [187] proposed an improvement on the XFEM approach suitable for structures with different materials, which is the case of adhesive joints. Their improvement consists in deflecting the crack propagation when it is expected to propagate from one material to another, much stiffer, material. To validate their model, they compared the strength predictions and crack paths of SLJ with several varying geometric parameters, namely adhesive fillet, round adherend corners, L_O and t_A. Their model showed strength predictions and crack paths very similar to the experimental results, with the crack propagating only in the adhesive. This methodology was also able to account for all the cited geometric changes. The predicted crack propagation for a straight corner is shown in Fig. 22b.

3.2.6. Meshless methods

Although meshless methods offer some advantages over FEM in fracture problems, such as eliminating the need of remeshing, their use in the strength prediction of adhesive joints has not been fully explored as of now. Different meshless methods are identified by their formulation, interpolation/approximation function and the integration scheme.
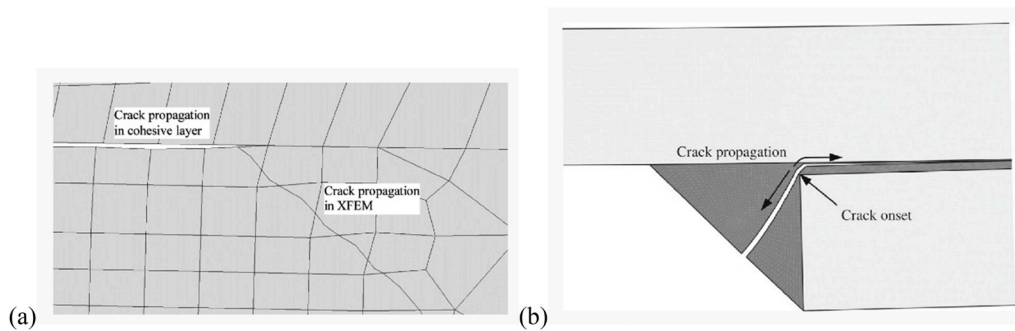
Fig. 22. Crack propagation, using the combined XFEM-CZM approach [97] (a) and using the Enhanced XFEM approach proposed by Stein et al. [187].

In this type of method, the nodal connectivity is achieved by the over-lapping of influence domains, as opposed to the elements of the FEM. The works described next are the sole found papers regarding the application of this technique to adhesive joints.

In 2014, Tsai et al. [188] proposed an approach that combined the symmetric smoothed particle hydrodynamics meshless method with CZM. They tested experimentally DCB specimens subjected to mode I, mode II and mixed-mode loadings, and compared those results with the developed numerical method. The results show that the strength pre-diction with the developed method, by a continuum mechanics approach, is very accurate for mode I and mixed-mode loadings, pro-vided that the mode I is dominant. The resulting load-displacement curves are also very close to the experimental ones. The Radial Point Interpolation Method (RPIM) was used by Bodjona and Lessard [189] to analyse hybrid bonded/bolted, adhesive and bolted composite SLJ. This work showed that the RPIM was able to correctly estimate the mid-thickness stress in the adhesive layer and that hybrid joints are stronger than either adhesive or bolted joints. Recently, Mubashar and Ashcroft [190] tested the capabilities of the Smoothed Particle Hydro-dynamics (SPH) meshless method implemented in the commercial software ABAQUS® when compared to the CZM implemented in the same software. Their results showed that the stress curves with the SPH method present big oscillations, and that the peel stresses are over predicted, while the shear stresses are under predicted. The load-displacement curve also presented some oscillations and the SPH under predicted the critical load by 9%, which was considered accept-able. The crack propagation path achieved in this work is shown in Fig. 23.

4. Critical discussion of the methods

This paper reviewed the different methods used to predict the strength of adhesive joints under static loading presented in literature from this decade. From the aforementioned discussion, it became clear that some methods have more potential and usability than others, that some methods have serious limitations which reduce their scope of applicability, and that others have margin to improve in the future,
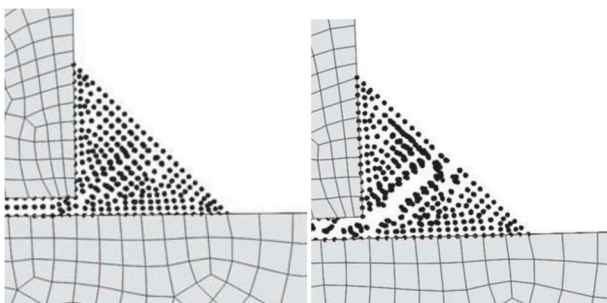

Fig. 23. Crack propagation using SPH [190].

making them more suitable for application to adhesive joints. The following discussion intends to describe the merits, limitations and suitability of each discussed method.

Analytical methods are the oldest way to predict the strength of a joint. They usually rely on closed-form solutions for stresses or strains, and they must be coupled with a failure criterion to predict the strength. These methods are often associated to fast output results and are mostly easy to program in a software for data analysis using a spreadsheet system, such as Microsoft Excel® or dedicated calculation and matrix manipulation software such as Matlab®. Apart from this, analytical methods are often used as a first trial in the design of adhesive joints. However, it should be noted that analytical formulations rely on simplifying assumptions that neglect particular issues of the joints' behaviour, such as elastic adhesives, elastic adherends, through-thickness stress simplifications and others. As a result, each analytical formulation is generally only able to predict the strength of a specific type of joint due to the differences between each joint type. For instance, methods that neglect adhesive plasticity can only give satisfactory pre-dictions for brittle adhesives, while joints with ductile adhesives result in under predictions with these criteria. On the other hand, these criteria tend to deviate further from the real joints' behaviour for large L_O [35]. Due to all these issues, the use of analytical techniques is nowadays limited.

Therefore, numerical methods have been the object of intense study in the strength prediction of adhesive joints due to their versatility. Numerical approaches in this work were divided into six different cat-egories, which are summarized as follows:

- Continuum mechanics provide the simplest approach by assessing joint failure by stress or strain parameters of the material, are easy to apply and do not require large computational resources. Compared to analytical methods, unlimited geometries can be modelled, and complex material behaviours can be easily implemented. However, this technique still disregards energetic concepts, which can be vital to obtain accurate strength predictions for ductile adhesives. More-over, the stress\strain singularity near the adherend/adhesive interface can cause a mesh dependency on the predictions without convergence being attained. Some recent criteria, like the CLS cri-terion, are able to overcome this deficiency by using the stresses/strains in the adhesive mid-thickness plane where there is no sin-gularity, but also requiring calibration with experimental data. In view of this discussion, continuum mechanics is notoriously a more refined technique than analytical methods, but its use in design should be exercised with caution.
- Fracture mechanics approaches enable the use of energetic concepts and criteria to simulate crack growth, which brings accurate modelling for all materials, ranging from brittle to ductile. However, these are traditionally limited to problems with an initial crack, such that the imposed criteria can propagate it. Thus, in pristine structures without initial defects, coalescence of cracks is not possible. Apart from this, unless specific algorithms are developed, continuous crack

growth is not contemplated, i.e., only the conditions for crack growth from a given damaged state is possible. These limitations are on the origin of a residual use of this technique for strength prediction of adhesive joints. An exception is the FFM, which was successfully applied to adhesive joints without initial cracks, being able to predict crack initiation and joint strength with good accuracy.

- Damage mechanics generally uses a damage parameter that gradually decreases material stiffness after a given stress/strain is achieved. This technique is able to account for different damage mechanisms, such as cohesive failure of the adhesive and adherend failure, including in composite laminates (in this specific case, the different failure modes occurring in composite materials can be modelled). These methods are also able to determine crack propagation through random paths and can provide accurate strength predictions in adhesive joints with arbitrary geometric and materials conditions. However, parameter calibration and the physical meaning of the damage variables used to depreciate the material properties can be complicated. Due to this limitation and to the uprising of techniques such as CZM, which promote crack growth with energetic principles (i.e., based on physically sound and measurable parameters), damage mechanics is not much widespread for strength prediction in adhesive joints.

- The works from this decade show that CZM are the joint strength prediction method that has been studied more extensively in academia, providing accurate strength predictions for a wide range of joints, due to being based on a mixed formulation, including continuum mechanics principles for damage initiation and fracture mechanics parameters for crack propagation. Actually, this technique is extremely powerful and accurate for adhesive joints with virtually any geometry and material characteristics. Moreover, it is possible to tailor the behaviour of the adhesive and eventually adherends with different CZM law shapes, which is particularly significant when modelling ductile materials, for which case the most common triangular CZM law cannot be the best solution. The method is also mesh insensitive, provided that enough integration points undergo softening simultaneously. As a result, this technique is recommended for the best results in adhesive joints' design. Nonetheless, two limitations arise with CZM. The first one is that this method usually requires the measurement of geometrically dependent adhesive properties. The second one is that CZM modelling requires to place the cohesive elements in potential fracture planes to enable crack propagation, i.e., if a failure path is not equated, damage modelling along that path is not included in the models. However, in adhesive joints, typically the potential fracture paths are easy to define beforehand, thus this limitation loses relevance.

- The XFEM was only recently used to study adhesive joints, but it shows some promise due to also relying on fracture concepts for crack growth. It excels fracture mechanics techniques by including continuum-based criteria for damage initiation and algorithms to partition solid elements and promote the nucleation and growth of cracks. This method is able to predict crack propagation through random paths, but in adhesive joints this sometimes results in the crack propagating from the adhesive to the adherends due to the criteria used for crack direction estimation, which is not consistent with the real behaviour. This occurrence mostly takes place in joints with large deformations and rotations of the adhesive layer (such as SLJ), and prevents total failure to occur. A recent improvement on the XFEM is able to deflect the crack when the stiffness of the material where the crack is present is lower than that of the material to where the crack is predicted to propagate. However, at this stage, the possibility of crack growth anywhere in the model is not a major advantage for adhesive joints. Thus, together with the pointed limitations, no clear advantage exists nowadays over CZM modelling.

- Meshless methods are advanced numerical techniques which are an alternative to the FEM. The use of these method to study adhesive joints is limited, but they could be adopted more extensively in the future. Since these methods do not require a mesh, it could be advantageous to used them with fracture and damage mechanics criteria, because they do not need to remesh to simulate crack propagation. Currently, they were already used in conjunction with the popular CZM [188], achieving accurate strength predictions. However, these methods are generally computationally slower than the FEM.

5. Conclusions

This work provided a review of the different method to predict the strength of adhesive joints and their application in recent years. The strength prediction methods were divided into two main categories: analytical methods and numerical methods. The merits, limitations and applicability to adhesive joints were discussed in section 4. The aforementioned discussion showed that analytical techniques, although having evolved through the years, are not the best option for adhesive joints' design. However, they can provide a starting point, or give a rough prediction. Most numerical method approaches presented here are coupled to FEA (Finite Element Analyses), with the exception of meshless methods. Continuum mechanics, fracture mechanics and damage mechanics, due to different reasons, are not currently much employed to adhesive joints. CZM, on the other hand, is the recommended method for adhesive joints' analysis on account of its intrinsic formulation characteristics, incorporating continuum mechanics and fracture mechanics principles to perform a detailed analysis of the fracture process. This allows the approach to be of much more general utility than conventional fracture mechanics. Studies demonstrated that it is possible to experimentally determine the appropriate cohesive zone parameters of an adhesive bond, and to incorporate them into FEA for excellent predictive capabilities. The XFEM is still a very recent method and requires further improvements to be able to be applied to adhesive joints, due to its inherent characteristics, e.g. cohesive crack growth in a thin adhesive strip confined between stiffer adherends. Meshless methods, although extensively tested in other engineering applications, are currently in a very embryonic stage in adhesive joints. Since these methods do not need a mesh, they could be used with fracture or damage mechanics criteria to predict joint strength with great advantage over the FEM, because they can simulate damage growth without needing to remesh.

The state-of-the-art discussion carried out in this review showed that numerical methods for the design of bonded structures have been fast evolving in recent years, throughout the different available approaches, and by the adaption of new ones to adhesive joints. From the current condition, new developments in this matter are expected, and a few research tendencies are discussed to increase the use of these tools. CZM, as the most widespread method for the analysis of adhesive joints, should be able to benefit from more effective and less time-consuming calibration tools that improve its usability in industrial applications. Moreover, the ready availability of this tool in commercial software with different law shapes and criteria for damage initiation and propagation could be a significant step towards mass use. XFEM is not fully developed yet for application in adhesive joints, and new formulations that could overcome the formerly discussed limitations would make it a more powerful method. The use of meshless methods for adhesive joints is still in the first steps, even if they have potential, thus, the incorporation of fracture or damage based criteria to simulate damage growth would definitely be a step forward to enable them to compete with the FEM using those approaches.

Acknowledgements

References

[1] Ebnesajjad S, Landrock AH. Adhesives Technology handbook. third ed. William Andrew Publishing; 2015. https://doi.org/10.1016/C2013-0-18392-4.

[2] He X. A review of finite element analysis of adhesively bonded joints. Int J Adhesion Adhes 2011;31:248–64. https://doi.org/10.1016/j.ijadhadh.2011.01.006.

[3] Adams RD. Strength predictions for lap joints, especially with composite adherends. A review. J Adhes 1989;30:219–42. https://doi.org/10.1080/00218468908048207.

[4] Sauer RA. A survey of computational models for adhesion. J Adhes 2016;92:81–120. https://doi.org/10.1080/00218464.2014.1003210.

[5] da Silva LFM, Dillard DA, Blackman B, Adams RD. Testing adhesive joints. Wiley-VCH Verlag & Co. KGaA; 2012. https://doi.org/10.1002/9783527647026.

[6] Chaves FJP, da Silva LFM, de Moura MFSF, Dillard DA, Esteves VHC. Fracture mechanics tests in adhesively bonded joints: a literature review. J Adhes 2014;90:955–92. https://doi.org/10.1080/00218464.2013.859075.

[7] Giannis S, Adams RD. Failure of elastomeric sealants under tension and shear: experiments and analysis. Int J Adhesion Adhes 2019;91:77–91. https://doi.org/10.1016/j.ijadhadh.2019.03.007.

[8] Jouan A, Constantinescu A. A critical comparison of shear tests for adhesive joints. Int J Adhesion Adhes 2018;84:63–79. https://doi.org/10.1016/j.ijadhadh.2018.02.035.

[9] Voloshin A, Arcan M. Pure shear moduli of unidirectional fibre-reinforced materials (FRM). Fibre Sci Technol 1980;13:125–34. https://doi.org/10.1016/0015-0568(80)90041-X.

[10] Spaggiari A, Castagnetti D, Dragoni E. Experimental tests on tubular bonded butt specimens: effect of relief grooves on tensile strength of the adhesive. J Adhes 2012;88:499–512. https://doi.org/10.1080/00218464.2012.660831.

[11] Ji G, Ouyang Z, Li G. Effects of bondline thickness on Mode-I nonlinear interfacial fracture of laminated composites: an experimental study. Compos B Eng 2013;47:1–7. https://doi.org/10.1016/j.compositesb.2012.10.048.

[12] Marzi S, Biel A, Stigh U. On experimental methods to investigate the effect of layer thickness on the fracture behavior of adhesively bonded joints. Int J Adhesion Adhes 2011;31:840–50. https://doi.org/10.1016/j.ijadhadh.2011.08.004.

[13] Quan D, Murphy N, Cardiff P, Ivankovic A. The intrinsic fracture property of a rubber-modified epoxy adhesive: geometrical transferability. Eng Fract Mech 2018;203:240–9. https://doi.org/10.1016/j.engfracmech.2018.04.035.

[14] Teixeira JMD, Campilho RDSG, da Silva FJG. Numerical assessment of the double-cantilever Beam and tapered double-cantilever Beam tests for the GIC determination of adhesive layers. J Adhes 2018;94:951–73. https://doi.org/10.1080/00218464.2017.1383905.

[15] Ji G, Ouyang Z, Li G. Local interface shear fracture of bonded steel joints with various bondline thicknesses. Exp Mech 2012;52:481–91. https://doi.org/10.1007/s11340-011-9507-y.

[16] Wang WX, Nakata M, Takao Y, Matsubara T. Experimental investigation on test methods for mode II interlaminar fracture testing of carbon fiber reinforced composites. Compos Part A Appl Sci Manuf 2009;40:1447–55. https://doi.org/10.1016/j.compositesa.2009.04.029.

[17] Blackman BRK, Kinloch AJ, Rodriguez-Sanchez FS, Teo WS. The fracture behaviour of adhesively-bonded composite joints: effects of rate of test and mode of loading. Int J Solids Struct 2012;49:1434–52. https://doi.org/10.1016/j.ijsolstr.2012.02.022.

[18] Toolabi M, Blackman BRK. Guidelines for selecting the dimensions of adhesively bonded end-loaded split joints: an approach based on numerical cohesive zone length. Eng Fract Mech 2018;203:250–65. https://doi.org/10.1016/j.engfracmech.2018.05.019.

[19] de Oliveira BMA, Campilho RDSG, Silva FJG, Rocha RJB. Comparison between the ENF and 4ENF fracture characterization tests to evaluate GIIC of bonded aluminium joints. J Adhes 2018;94:910–31. https://doi.org/10.1080/00218464.2017.1387056.

[20] Hasegawa K, Crocombe AD, Coppuck F, Jewel D, Maher S. Characterising bonded joints with a thick and flexible adhesive layer-Part 1: fracture testing and behaviour. Int J Adhesion Adhes 2015;63:124–31. https://doi.org/10.1016/j.ijadhadh.2015.09.003.

[21] Costa M, Carbas R, Marques E, Viana G, da Silva LFM. An apparatus for mixed-mode fracture characterization of adhesive joints. Theor Appl Fract Mech 2017;91:94–102. https://doi.org/10.1016/j.tafmec.2017.04.014.

[22] Sadeghi MZ, Zimmermann J, Gabener A, Schroeder KU. The applicability of J-integral approach in the determination of mixed-mode fracture energy in a ductile adhesive. Int J Adhesion Adhes 2018;83:2–8. https://doi.org/10.1016/j.ijadhadh.2018.02.027.

[23] da Silva LFM, das Neves PJC, Adams RD, Spelt JK. Analytical models of adhesively bonded joints-Part I: literature survey. Int J Adhesion Adhes 2009;29:319–30. https://doi.org/10.1016/j.ijadhadh.2008.06.005.

[24] da Silva LFM, das Neves PJC, Adams RD, Wang A, Spelt JK. Analytical models of adhesively bonded joints-Part II: comparative study. Int J Adhesion Adhes 2009;29:331–41. https://doi.org/10.1016/j.ijadhadh.2008.06.007.

[25] Volkersen O. Die Nietkraftverteilung in zugbeanspruchten Nietverbindungen mit konstanten Laschenquerschnitten. Luftfahrtfor Schung 1938;15:41–7.

[26] Goland M, Reissner E. The stresses in cemented joints. J Appl Mech 1944;17:66.

[27] Campilho RDSG. Strength prediction of adhesively-bonded joints. CRC Press; 2017.

[28] Dragoni E, Goglio L, Kleiner F. Designing bonded joints by means of the JointCalc software. Int J Adhesion Adhes 2010;30:267–80. https://doi.org/10.1016/j.ijadhadh.2009.11.002.

[29] Zhao B, Lu ZH, Lu YN. Two-dimensional analytical solution of elastic stresses for balanced single-lap joints - variational method. Int J Adhesion Adhes 2014;49:115–26. https://doi.org/10.1016/j.ijadhadh.2013.12.026.

[30] Weißgraeber P, Stein N, Becker W. A general sandwich-type model for adhesive joints with composite adherends. Int J Adhesion Adhes 2014;55:56–63. https://doi.org/10.1016/j.ijadhadh.2014.06.009.

[31] Yousefsani SA, Tahani M. Analytical solutions for adhesively bonded composite single-lap joints under mechanical loadings using full layerwise theory. Int J Adhesion Adhes 2013;43:32–41. https://doi.org/10.1016/j.ijadhadh.2013.01.012.

[32] Icardi U, Sola F. Analysis of bonded joints with laminated adherends by a variable kinematics layerwise model. Int J Adhesion Adhes 2014;50:244–54. https://doi.org/10.1016/j.ijadhadh.2014.02.003.

[33] Wu XF, Zhao Y. Stress-function variational method for interfacial stress analysis of adhesively bonded joints. Int J Solids Struct 2013;50:4305–19. https://doi.org/10.1016/j.ijsolstr.2013.09.002.

[34] Yousefsani SA, Tahani M. Accurate determination of stress distributions in adhesively bonded homogeneous and heterogeneous double-lap joints. Eur J Mech A Solid 2013;39:197–208. https://doi.org/10.1016/j.euromechsol.2012.12.001.

[35] De Sousa CCRG, Campilho RRDSG, Marques EAS, Costa M, Da Silva LFM. Overview of different strength prediction techniques for single-lap bonded joints. Proc Inst Mech Eng L J Mater Des Appl 2017;231:210–23. https://doi.org/10.1177/1464420716675746.

[36] Hart-Smith L J. Adhesive-bonded single lap joints. 1973.

[37] Crocombe AD. Global yielding as a failure criterion for bonded joints. Int J Adhesion Adhes 1989;9:145–53. https://doi.org/10.1016/0143-7496(89)90110-3.

[38] Moradi A, Leguillon D, Carrère N. Influence of the adhesive thickness on a debonding – an asymptotic model. Eng Fract Mech 2013;114:55–68. https://doi.org/10.1016/j.engfracmech.2013.10.008.

[39] Weißgraeber P, Becker W. Finite Fracture Mechanics model for mixed mode fracture in adhesive joints. Int J Solids Struct 2013;50:2383–94. https://doi.org/10.1016/j.ijsolstr.2013.03.012.

[40] Ojalvo IU, Eidinoff HL. Bond thickness effects upon stresses in single-lap adhesive joints. AIAA J 1978;16:204–11. https://doi.org/10.2514/3.60878.

[41] Stein N, Weißgraeber P, Becker W. A model for brittle failure in adhesive lap joints of arbitrary joint configuration. Compos Struct 2015;133:707–18. https://doi.org/10.1016/j.compstruct.2015.07.100.

[42] Stein N, Felger J, Becker W. Analytical models for functionally graded adhesive single lap joints: a comparative study. Int J Adhesion Adhes 2017;76:70–82. https://doi.org/10.1016/j.ijadhadh.2017.02.001.

[43] Carbas RJC, Da Silva LFM, Madureira ML, Critchlow GW. Modelling of functionally graded adhesive joints. J Adhes 2014;90:698–716. https://doi.org/10.1080/00218464.2013.834255.

[44] Stein N, Mardani H, Becker W. An efficient analysis model for functionally graded adhesive single lap joints. Int J Adhesion Adhes 2016;70:117–25. https://doi.org/10.1016/j.ijadhadh.2016.06.001.

[45] Stein N, Weißgraeber P, Becker W. Stress solution for functionally graded adhesive joints. Int J Solids Struct 2016;97_98:300–11. https://doi.org/10.1016/j.ijsolstr.2016.07.019.

[46] Carbas RJC, Da Silva LFM, Critchlow GW. Adhesively bonded functionally graded joints by induction heating. Int J Adhesion Adhes 2014;48:110–8. https://doi.org/10.1016/j.ijadhadh.2013.09.045.

[47] Anyfantis KN, Tsouvalis NG. A novel traction-separation law for the prediction of the mixed mode response of ductile adhesive joints. Int J Solids Struct 2012;49:213–26. https://doi.org/10.1016/j.ijsolstr.2011.10.001.

[48] Liu Y, Lemanski S, Zhang X. Parametric study of size, curvature and free edge effects on the predicted strength of bonded composite joints. Compos Struct 2018;202:364–73. https://doi.org/10.1016/j.compstruct.2018.02.017.

[49] Ribeiro FL, Borges L, Dalmeida JRM. Numerical stress analysis of carbon-fibre-reinforced epoxy composite single-lap joints. Int J Adhesion Adhes 2011;31:331–7. https://doi.org/10.1016/j.ijadhadh.2011.01.008.

[50] Tsouvalis NG, Karatzas VA. An investigation of the tensile strength of a composite-to-metal adhesive joint. Appl Compos Mater 2011;18:149–63. https://doi.org/10.1007/s10443-010-9137-z.

[51] Ozel A, Yazici B, Akpinar S, Aydin MD, Temiz Ş. A study on the strength of adhesively bonded joints with different adherends. Compos B Eng 2014;62:167–74. https://doi.org/10.1016/j.compositesb.2014.03.001.

[52] Gültekin K, Akpinar S, Özel A, Öner GA. Effects of unbalance on the adhesively bonded composites-aluminium joints. J Adhes 2017;93:674–87. https://doi.org/10.1080/00218464.2015.1136998.

[53] Adin H. The investigation of the effect of angle on the failure load and strength of scarf lap joints. Int J Mech Sci 2012;61:24–31. https://doi.org/10.1016/J.IJMECSCI.2012.04.010.

[54] Goglio L, Rossetto M, Dragoni E. Design of adhesive joints based on peak elastic stresses. Int J Adhesion Adhes 2008;28:427–35. https://doi.org/10.1016/j.ijadhadh.2008.04.001.

[55] Ayatollahi MR, Akhavan-Safar A. Failure load prediction of single lap adhesive joints based on a new linear elastic criterion. Theor Appl Fract Mech 2015;80:210–7. https://doi.org/10.1016/j.tafmec.2015.07.013.

[56] Taylor D. The theory of critical distances. Eng Fract Mech 2008;75:1696–705. https://doi.org/10.1016/j.engfracmech.2007.04.007.

[57] Akhavan-Safar A, Ayatollahi MR, da Silva LFM. Strength prediction of adhesively bonded single lap joints with different bondline thicknesses: a critical longitudinal strain approach. Int J Solids Struct 2017;109:189–98. https://doi.org/10.1016/j.ijsolstr.2017.01.022.

[58] Khoramishad H, Akhavan-Safar A, Ayatollahi MR, Da Silva LFM. Predicting static strength in adhesively bonded single lap joints using a critical distance based method: substrate thickness and overlap length effects. Proc Inst Mech Eng L J Mater Des Appl 2017;231:237–46. https://doi.org/10.1177/1464420716666427.

[59] Akhavan-Safar A, da Silva LFM, Ayatollahi MR. An investigation on the strength of single lap adhesive joints with a wide range of materials and dimensions using a critical distance approach. Int J Adhesion Adhes 2017;78:248–55. https://doi.org/10.1016/j.ijadhadh.2017.08.009.

[60] Razavi SMJ, Ayatollahi MR, Majidi HR, Berto F. A strain-based criterion for failure load prediction of steel/CFRP double strap joints. Compos Struct 2018;206:116–23. https://doi.org/10.1016/j.compstruct.2018.08.046.

[61] Karachalios EF, Adams RD, da Silva LFM. Single lap joints loaded in tension with high strength steel adherends. Int J Adhesion Adhes 2013;43:81–95. https://doi.org/10.1016/j.ijadhadh.2013.01.016.

[62] Karachalios EF, Adams RD, da Silva LFM. Single lap joints loaded in tension with ductile steel adherends. Int J Adhesion Adhes 2013;43:96–108. https://doi.org/10.1016/j.ijadhadh.2013.01.017.

[63] Karachalios EF, Adams RD, Da Silva LFM. The behaviour of single lap joints under bending loading. J Adhes Sci Technol 2013;27:1811–27. https://doi.org/10.1080/01694243.2012.761926.

[64] Zhao X, Adams RD, Da Silva LFM. Single lap joints with rounded adherend corners: stress and strain analysis. J Adhes Sci Technol 2011;25:819–36. https://doi.org/10.1163/016942410X520871.

[65] Zhao X, Adams RD, Da Silva LFM. Single lap joints with rounded adherend corners: experimental results and strength prediction. J Adhes Sci Technol 2011;25:837–56. https://doi.org/10.1163/016942410X520880.

[66] Reis PNB, Ferreira JAM, Antunes F. Effect of adherends rigidity on the shear strength of single lap adhesive joints. Int J Adhesion Adhes 2011;31:193–201. https://doi.org/10.1016/j.ijadhadh.2010.12.003.

[67] Campilho RDSG, Pinto AMG, Banea MD, Silva RF, Da Silva LFM. Strength improvement of adhesively-bonded joints using a reverse-bent geometry. J Adhes Sci Technol 2011;25:2351–68. https://doi.org/10.1163/016942411X580081.

[68] Wu C, Chen C, He L, Yan W. Comparison on damage tolerance of scarf and stepped-lap bonded composite joints under quasi-static loading. Compos B Eng 2018;155:19–30. https://doi.org/10.1016/j.compositesb.2018.08.031.

[69] da Silva LFM, Campilho RDSG. Advances in numerical modeling of adhesive joints. Springer; 2012. https://doi.org/10.1007/978-3-642-23608-2.

[70] Rice JR. A path independent integral and the approximate analysis of strain concentration by notches and cracks. J Appl Mech 1968;35:379. https://doi.org/10.1115/1.3601206.

[71] Rybicki EF, Kanninen MF. A finite element calculation of stress intensity factors by a modified crack closure integral. Eng Fract Mech 1977;9:931–8. https://doi.org/10.1016/0013-7944(77)90013-3.

[72] Chen Z, Adams RD, Da Silva LFM. Prediction of crack initiation and propagation of adhesive lap joints using an energy failure criterion. Eng Fract Mech 2011;78:990–1007. https://doi.org/10.1016/j.engfracmech.2010.12.004.

[73] Afendi M, Teramoto T, Bakri H Bin. Strength prediction of epoxy adhesively bonded scarf joints of dissimilar adherends. Int J Adhesion Adhes 2011;31:402–11. https://doi.org/10.1016/j.ijadhadh.2011.03.001.

[74] Goh JY, Georgiadis S, Orifici AC, Wang CH. Effects of bondline flaws on the damage tolerance of composite scarf joints. Compos Part A Appl Sci Manuf 2013;55:110–9. https://doi.org/10.1016/j.compositesa.2013.07.017.

[75] Cameselle-Molares A, Sarfaraz R, Shahverdi M, Keller T, Vassilopoulos AP. Fracture mechanics-based progressive damage modelling of adhesively bonded fibre-reinforced polymer joints. Fatigue Fract Eng Mater Struct 2017;40:2183–93. https://doi.org/10.1111/ffe.12647.

[76] Akhavan-Safar A, Ayatollahi MR, Rastegar S, da Silva LFM. Residual static strength and the fracture initiation path in adhesively bonded joints weakened with interfacial edge pre-crack. J Adhes Sci Technol 2018;32:2019–40. https://doi.org/10.1080/01694243.2018.1458812.

[77] Leguillon D. Strength or toughness? A criterion for crack onset at a notch. Eur J Mech A Solid 2002;21:61–72. https://doi.org/10.1016/S0997-7538(01)01184-6.

[78] Ernesto Mendoza-Navarro L, Diaz-Diaz A, Castañeda-Balderas R, Hunkeler S, Noret R. Interfacial failure in adhesive joints: experiments and predictions. Int J Adhesion Adhes 2013;44:36–47. https://doi.org/10.1016/j.ijadhadh.2013.02.004.

[79] Moradi A, Carrère N, Leguillon D, Martin E, Cognard JY. Strength prediction of bonded assemblies using a coupled criterion under elastic assumptions: effect of material and geometrical parameters. Int J Adhesion Adhes 2013;47:73–82. https://doi.org/10.1016/j.ijadhadh.2013.09.044.

[80] Hell S, Weißgraeber P, Felger J, Becker W. A coupled stress and energy criterion for the assessment of crack initiation in single lap joints: a numerical approach.

[81] Carrere N, Martin E, Leguillon D. Comparison between models based on a coupled criterion for the prediction of the failure of adhesively bonded joints. Eng Fract Mech 2015;138:185–201. https://doi.org/10.1016/j.engfracmech.2015.03.004.

[82] Doitrand A, Leguillon D. 3D application of the coupled criterion to crack initiation prediction in epoxy/aluminum specimens under four point bending. Int J Solids Struct 2018;143:175–82. https://doi.org/10.1016/j.ijsolstr.2018.03.005.

[83] Doitrand A, Leguillon D. Comparison between 2D and 3D applications of the coupled criterion to crack initiation prediction in scarf adhesive joints. Int J Adhesion Adhes 2018;85:69–76. https://doi.org/10.1016/j.ijadhadh.2018.05.022.

[84] Le Pavic J, Stamoulis G, Bonnemains T, Da Silva D, Thévenet D. Fast failure prediction of adhesively bonded structures using a coupled stress-energetic failure criterion. Fatigue Fract Eng Mater Struct 2019;42:627–39. https://doi.org/10.1111/ffe.12938.

[85] Weißgraeber P, Leguillon D, Becker W. A review of Finite Fracture Mechanics: crack initiation at singular and non-singular stress raisers. Arch Appl Mech 2016;86:375–401. https://doi.org/10.1007/s00419-015-1091-7.

[86] Weißgraeber P, Felger J, Talmon l'Armée A, Becker W. Crack initiation in single lap joints: effects of geometrical and material properties. Int J Fract 2015;192:155–66. https://doi.org/10.1007/s10704-015-9992-6.

[87] García JA, Chiminelli A, García B, Lizaranzu M, Jiménez MA. Characterization and material model definition of toughened adhesives for finite element analysis. Int J Adhesion Adhes 2011;31:182–92. https://doi.org/10.1016/j.ijadhadh.2010.12.006.

[88] Chousal JAG, De Moura MFSF. Mixed-mode I+II continuum damage model applied to fracture characterization of bonded joints. Int J Adhesion Adhes 2013;41:92–7. https://doi.org/10.1016/j.ijadhadh.2012.10.014.

[89] Stapleton SE, Pineda EJ, Gries T, Waas AM. Adaptive shape functions and internal mesh adaptation for modeling progressive failure in adhesively bonded joints. Int J Solids Struct 2014;51:3252–64. https://doi.org/10.1016/j.ijsolstr.2014.05.022.

[90] Stapleton SE, Waas AM, Bednarcyk BA. Modeling progressive failure of bonded joints using a single joint finite element. AIAA J 2011;49:1740–9. https://doi.org/10.2514/1.J050889.

[91] Belnoue JP-HPH, Hallett SR. Cohesive/adhesive failure interaction in ductile adhesive joints Part I: a smeared-crack model for cohesive failure. Int J Adhesion Adhes 2016;68:359–68. https://doi.org/10.1016/j.ijadhadh.2016.03.009.

[92] Belnoue JPH, Giannis S, Dawson M, Hallett SR. Cohesive/adhesive failure interaction in ductile adhesive joints Part II: quasi-static and fatigue analysis of double lap-joint specimens subjected to through-thickness compressive loading. Int J Adhesion Adhes 2016;68:369–78. https://doi.org/10.1016/j.ijadhadh.2016.03.010.

[93] Sugiman S, Ahmad H. Comparison of cohesive zone and continuum damage approach in predicting the static failure of adhesively bonded single lap joints. J Adhes Sci Technol 2017;31:552–70. https://doi.org/10.1080/01694243.2016.1222048.

[94] Riccio A, Ricchiuto R, Di Caprio F, Sellitto A, Raimondo A. Numerical investigation of constitutive material models on bonded joints in scarf repaired composite laminates. Eng Fract Mech 2017;173:91–106. https://doi.org/10.1016/j.engfracmech.2017.01.003.

[95] Zhang Q, Cheng X, Cheng Y, Li W, Hu R. Investigation of tensile behavior and influence factors of composite-to-metal 2D-scarf bonded joint. Eng Struct 2019;180:284–94. https://doi.org/10.1016/j.engstruct.2018.11.036.

[96] Kim MH, Hong HS. An adaptation of mixed-mode I + II continuum damage model for prediction of fracture characteristics in adhesively bonded joint. Int J Adhesion Adhes 2018;80:87–103. https://doi.org/10.1016/j.ijadhadh.2017.10.008.

[97] Mubashar A, Ashcroft IA, Crocombe AD. Modelling damage and failure in adhesive joints using a combined XFEM-cohesive element methodology. J Adhes 2014;90:682–97. https://doi.org/10.1080/00218464.2013.826580.

[98] Stuparu F, Constantinescu DM, Apostol DA, Sandu M. A combined cohesive elements - XFEM approach for analyzing crack propagation in bonded joints. J Adhes 2016;92:535–52. https://doi.org/10.1080/00218464.2015.1115355.

[99] Imanaka M, Omiya M, Taguchi N. Estimation of static strength of adhesively bonded single lap joints with an acrylic adhesive under tensile shear condition based on cohesive zone model. J Adhes Sci Technol 2019;0:1–15. https://doi.org/10.1080/01694243.2018.1548550.

[100] Jung Lee M, Min Cho T, Seock Kim W, Chai Lee B, Ju Lee J. Determination of cohesive parameters for a mixed-mode cohesive zone model. Int J Adhesion Adhes 2010;30:322–8. https://doi.org/10.1016/j.ijadhadh.2009.10.005.

[101] Kim YT, Lee MJ, Lee BC. Simulation of adhesive joints using the superimposed finite element method and a cohesive zone model. Int J Adhesion Adhes 2011;31:357–62. https://doi.org/10.1016/j.ijadhadh.2010.11.015.

[102] Liao L, Sawa T, Huang C. Numerical analysis on load-bearing capacity and damage of double scarf adhesive joints subjected to combined loadings of tension and bending. Int J Adhesion Adhes 2014;53:65–71. https://doi.org/10.1016/j.ijadhadh.2014.01.010.

[103] Floros IS, Tserpes KI, Löbel T. Mode-I, mode-II and mixed-mode I+II fracture behavior of composite bonded joints: experimental characterization and numerical simulation. Compos B Eng 2015;78:459–68. https://doi.org/10.1016/j.compositesb.2015.04.006.

[104] Stuparu FA, Apostol DA, Constantinescu DM, Picu CR, Sandu M, Sorohan S. Local evaluation of adhesive failure in similar and dissimilar single-lap joints. Eng Fract Mech 2017;183:39–52. https://doi.org/10.1016/j.engfracmech.2017.05.029.

[105] Matta S, Ramji M. Prediction of mechanical behaviour of adhesively bonded CFRP scarf jointed specimen under tensile loading using localised DIC and CZM. Int J Adhesion Adhes 2019;89:88–108. https://doi.org/10.1016/j.ijadhadh.2018.12.002.

[106] Barenblatt G. The formation of equilibrium cracks during brittle fracture. General ideas and hypotheses. Axially-symmetric cracks. J Appl Math Mech 1959;23: 622–36. https://doi.org/10.1016/0021-8928(59)90157-1.

[107] Dugdale DS. Yielding of steel sheets containing slits. J Mech Phys Solids 1960;8: 100–4. https://doi.org/10.1016/0022-5096(60)90013-2.

[108] Rocha RJB, Campilho RDSG. Evaluation of different modelling conditions in the cohesive zone analysis of single-lap bonded joints. J Adhes 2018;94:562–82. https://doi.org/10.1080/00218464.2017.1307107.

[109] Li G, Li C. Assessment of debond simulation and cohesive zone length in a bonded composite joint. Compos B Eng 2015;69:359–68. https://doi.org/10.1016/j.compositesb.2014.10.024.

[110] Álvarez D, Blackman BRK, Guild FJ, Kinloch AJ. Mode I fracture in adhesively-bonded joints: a mesh-size independent modelling approach using cohesive elements. Eng Fract Mech 2014;115:73–95. https://doi.org/10.1016/j.engfracmech.2013.10.005.

[111] Campilho RDSG, Banea MD, Pinto AMG, Da Silva LFM, De Jesus AMP. Strength prediction of single- and double-lap joints by standard and extended finite element modelling. Int J Adhesion Adhes 2011;31:363–72. https://doi.org/10.1016/j.ijadhadh.2010.09.008.

[112] O'Mahoney DC, Katnam KB, O'Dowd NP, McCarthy CT, Young TM. Taguchi analysis of bonded composite single-lap joints using a combined interface-adhesive damage model. Int J Adhesion Adhes 2013;40:168–78. https://doi.org/10.1016/j.ijadhadh.2012.06.001.

[113] Sugiman S, Crocombe AD, Aschroft IA. Modelling the static response of unaged adhesively bonded structures. Eng Fract Mech 2013;98:296–314. https://doi.org/10.1016/j.engfracmech.2012.10.014.

[114] Heshmati M, Haghani R, Al-Emrani M, André A. On the strength prediction of adhesively bonded FRP-steel joints using cohesive zone modelling. Theor Appl Fract Mech 2018;93:64–78. https://doi.org/10.1016/j.tafmec.2017.06.022.

[115] Geleta TN, Woo K, Cairns DS, Samborsky D. Failure behavior of inclined thick adhesive joints with manufacturing defect. J Mech Sci Technol 2018;32:2173–82. https://doi.org/10.1007/s12206-018-0426-z.

[116] Neumayer J, Koerber H, Hinterhölzl R. An explicit cohesive element combining cohesive failure of the adhesive and delamination failure in composite bonded joints. Compos Struct 2016;146:75–83. https://doi.org/10.1016/j.compstruct.2016.03.009.

[117] Ye J, Yan Y, Li J, Hong Y, Tian Z. 3D explicit finite element analysis of tensile failure behavior in adhesive-bonded composite single-lap joints. Compos Struct 2018;201:261–75. https://doi.org/10.1016/j.compstruct.2018.05.134.

[118] Campilho RDSG, Banea MD, Neto JABP, Da Silva LFM. Modelling adhesive joints with cohesive zone models: effect of the cohesive law shape of the adhesive layer. Int J Adhesion Adhes 2013;44:48–56. https://doi.org/10.1016/j.ijadhadh.2013.02.006.

[119] Carvalho UTF, Campilho RDSG. Validation of pure tensile and shear cohesive laws obtained by the direct method with single-lap joints. Int J Adhesion Adhes 2017;77:41–50. https://doi.org/10.1016/j.ijadhadh.2017.04.002.

[120] Anyfantis KN. On the failure analysis of bondlines: stress or energy based fracture criteria? Eng Fract Mech 2014;126:108–25. https://doi.org/10.1016/j.engfracmech.2014.04.024.

[121] Karac A, Blackman BRK, Cooper V, Kinloch AJ, Rodriguez Sanchez S, Teo WS, et al. Modelling the fracture behaviour of adhesively-bonded joints as a function of test rate. Eng Fract Mech 2011;78:973–89. https://doi.org/10.1016/j.engfracmech.2010.11.014.

[122] Neto JABP, Campilho RDSG, Da Silva LFM. Parametric study of adhesive joints with composites. Int J Adhesion Adhes 2012;37:96–101. https://doi.org/10.1016/j.ijadhadh.2012.01.019.

[123] Fernandes RL, Campilho RDSG. Testing different cohesive law shapes to predict damage growth in bonded joints loaded in pure tension. J Adhes 2017;93:57–76. https://doi.org/10.1080/00218464.2016.1169176.

[124] Fernandes RL, Campilho RGSG. Accuracy of cohesive laws with different shape for the shear behaviour prediction of bonded joints. J Adhes 2018;00:1–23. https://doi.org/10.1080/00218464.2018.1438895.

[125] Carvalho UTF, Campilho RDSG. Application of the direct method for cohesive law estimation applied to the strength prediction of double-lap joints. Theor Appl Fract Mech 2016;85:140–8. https://doi.org/10.1016/j.tafmec.2016.08.018.

[126] Zhang J, Wang J, Yuan Z, Jia H. Effect of the cohesive law shape on the modelling of adhesive joints bonded with brittle and ductile adhesives. Int J Adhesion Adhes 2018;85:37–43. https://doi.org/10.1016/j.ijadhadh.2018.05.017.

[127] Park K, Paulino GH, Roesler JR. A unified potential-based cohesive model of mixed-mode fracture. J Mech Phys Solids 2009;57:891–908. https://doi.org/10.1016/j.jmps.2008.10.003.

[128] Alfano M, Furgiuele F, Lubineau G, Paulino GH. Simulation of debonding in Al/epoxy T-peel joints using a potential-based cohesive zone model. Procedia Eng 2011;10:1760–5. https://doi.org/10.1016/j.proeng.2011.04.293.

[129] Alfano M, Lubineau G, Furgiuele F, Paulino GH. On the enhancement of bond toughness for Al/epoxy T-peel joints with laser treated substrates. Int J Fract 2011;171:139–50. https://doi.org/10.1007/s10704-011-9636-4.

[130] Anyfantis KN. Finite element predictions of composite-to-metal bonded joints with ductile adhesive materials. Compos Struct 2012;94:2632–9. https://doi.org/10.1016/j.compstruct.2012.03.002.

[131] Anyfantis KN, Tsouvalis NG. Loading and fracture response of CFRP-to-steel adhesively bonded joints with thick adherents – Part II: numerical simulation.

[132] Anyfantis KN, Tsouvalis NG. A 3D ductile constitutive mixed-mode model of cohesive elements for the finite element analysis of adhesive joints. J Adhes Sci Technol 2013;27:1146–78. https://doi.org/10.1080/01694243.2012.735900.

[133] Anyfantis KN, Tsouvalis NG. Analysis of an adhesively bonded single lap joint subjected to eccentric loading. Int J Adhesion Adhes 2013;41:41–9. https://doi.org/10.1016/j.ijadhadh.2012.10.007.

[134] Xu Y, Guo Y, Liang L, Liu Y, Wang X. A unified cohesive zone model for simulating adhesive failure of composite structures and its parameter identification. Compos Struct 2017;182:555–65. https://doi.org/10.1016/j.compstruct.2017.09.012.

[135] Shen B, Paulino GH. Direct extraction of cohesive fracture properties from digital image correlation: a hybrid inverse technique. Exp Mech 2011;51:143–63. https://doi.org/10.1007/s11340-010-9342-6.

[136] Ji G, Ouyang Z, Li G, Ibekwe S, Pang SS. Effects of adhesive thickness on global and local mode-I interfacial fracture of bonded joints. Int J Solids Struct 2010;47: 2445–58. https://doi.org/10.1016/j.ijsolstr.2010.05.006.

[137] Carlberger T, Stigh U. Influence of layer thickness on cohesive properties of an epoxy-based adhesive-an experimental study. J Adhes 2010;86:814–33. https://doi.org/10.1080/00218464.2010.498718.

[138] da Silva LFM, de Magalhães FACRG, Chaves FJP, De Moura MFSF. Mode II fracture toughness of a brittle and a ductile adhesive as a function of the adhesive thickness. J Adhes 2010;86:889–903. https://doi.org/10.1080/00218464.2010.506155.

[139] Boutar Y, Naïmi S, Mezlini S, da Silva LFM, Ben Sik Ali M. Characterization of aluminium one-component polyurethane adhesive joints as a function of bond thickness for the automotive industry: fracture analysis and behavior. Eng Fract Mech 2017;177:45–60. https://doi.org/10.1016/J.ENGFRACMECH.2017.03.044.

[140] Ji G, Ouyang Z, Li G. On the interfacial constitutive laws of mixed mode fracture with various adhesive thicknesses. Mech Mater 2012;47:24–32. https://doi.org/10.1016/j.mechmat.2012.01.002.

[141] Figueiredo JCP, Campilho RDSG, Marques EAS, Machado JJM, da Silva LFM. Adhesive thickness influence on the shear fracture toughness measurements of adhesive joints. Int J Adhesion Adhes 2018;83:15–23. https://doi.org/10.1016/j.ijadhadh.2018.02.015.

[142] Liao L, Huang C, Sawa T. Effect of adhesive thickness, adhesive type and scarf angle on the mechanical properties of scarf adhesive joints. Int J Solids Struct 2013;50:4333–40. https://doi.org/10.1016/j.ijsolstr.2013.09.005.

[143] Xu W, Wei Y. Influence of adhesive thickness on local interface fracture and overall strength of metallic adhesive bonding structures. Int J Adhesion Adhes 2013;40:158–67. https://doi.org/10.1016/j.ijadhadh.2012.07.012.

[144] Demiral M, Kadioglu F. Failure behaviour of the adhesive layer and angle ply composite adherends in single lap joints : a numerical study. Int J Adhesion Adhes 2018;87:181–90. https://doi.org/10.1016/j.ijadhadh.2018.10.010.

[145] Martiny P, Lani F, Kinloch AJ, Pardoen T. Numerical analysis of the energy contributions in peel tests: a steady-state multilevel finite element approach. Int J Adhesion Adhes 2008;28:222–36. https://doi.org/10.1016/j.ijadhadh.2007.06.005.

[146] Martiny P, Lani F, Kinloch AJ, Pardoen T. A multiscale parametric study of mode I fracture in metal-to-metal low-toughness adhesive joints. Int J Fract 2012;173: 105–33. https://doi.org/10.1007/s10704-011-9667-x.

[147] Pardoen T, Ferracin T, Landis CM, Delannay F. Constraint effects in adhesive joint fracture. J Mech Phys Solids 2005;53:1951–83. https://doi.org/10.1016/j.jmps.2005.04.009.

[148] Azevedo JCS, Campilho RDSG, da Silva FJG, Faneco TMS, Lopes RM. Cohesive law estimation of adhesive joints in mode II condition. Theor Appl Fract Mech 2015;80:143–54. https://doi.org/10.1016/j.tafmec.2015.09.007.

[149] Ridha M, Tan VBCC, Tay TE. Traction – separation laws for progressive failure of bonded scarf repair of composite panel. Compos Struct 2011;93:1239–45. https://doi.org/10.1016/j.compstruct.2010.10.015.

[150] Campilho RDSG, Banea MD, Neto JABP, Da Silva LFM. Modelling of single-lap joints using cohesive zone models: effect of the cohesive parameters on the output of the simulations. J Adhes 2012;88:513–33. https://doi.org/10.1080/00218464.2012.660834.

[151] Fernández-Cañadas LM, Iváñez I, Sanchez-Saez S. Influence of the cohesive law shape on the composite adhesively-bonded patch repair behaviour. Compos B Eng 2016;91:414–21. https://doi.org/10.1016/j.compositesb.2016.01.056.

[152] Fernandes RL, De Moura MFSF, Moreira RDF. Effect of temperature on pure modes I and II fracture behavior of composite bonded joints. Compos B Eng 2016; 96:35–44. https://doi.org/10.1016/j.compositesb.2016.04.022.

[153] Santos MAS, Campilho RDSG. Mixed-mode fracture analysis of composite bonded joints considering adhesives of different ductility. Int J Fract 2017;207:55–71. https://doi.org/10.1007/s10704-017-0219-x.

[154] Nunes FAA, Campilho RDSG. Mixed-mode fracture analysis of adhesively-bonded joints using the ATDCB test specimen. Int J Adhesion Adhes 2018;85:58–68. https://doi.org/10.1016/j.ijadhadh.2018.05.019.

[155] Nunes SLS, Campilho RDSG, Da Silva FJG, De Sousa CCRG, Fernandes TAB, Banea MD, et al. Comparative failure assessment of single and double lap joints with varying adhesive systems. J Adhes 2016;92:610–34. https://doi.org/10.1080/00218464.2015.1103227.

[156] Fernandes TAB, Campilho RDSG, Banea MD, Da Silva LFM. Adhesive selection for single lap bonded joints: experimentation and advanced techniques for strength prediction. J Adhes 2015;91:841–62. https://doi.org/10.1080/00218464.2014.994703.

Compos Struct 2013;96:858–68. https://doi.org/10.1016/j.compstruct.2012.08.056.

[157] Moreira RDF, Campilho RDSG. Strength improvement of adhesively-bonded scarf repairs in aluminium structures with external reinforcements. Eng Struct 2015; 101:99–110. https://doi.org/10.1016/j.engstruct.2015.07.001.

[158] Li J, Yan Y, Liang Z, Zhang T. Experimental and numerical study of adhesively bonded CFRP scarf-lap joints subjected to tensile loads. J Adhes 2016;92:1–17. https://doi.org/10.1080/00218464.2014.987343.

[159] Carneiro MAS, Campilho RDSG. Analysis of adhesively-bonded T-joints by experimentation and cohesive zone models. J Adhes Sci Technol 2017;31: 1998–2014. https://doi.org/10.1080/01694243.2017.1291320.

[160] Ji YM, Han KS. Fracture mechanics approach for failure of adhesive joints in wind turbine blades. Renew Energy 2014;65:23–8. https://doi.org/10.1016/j.renene.2013.07.004.

[161] Garrido M, Correia JR, Keller T, Branco FA. Adhesively bonded connections between composite sandwich floor panels for building rehabilitation. Compos Struct 2015;134:255–68. https://doi.org/10.1016/J.COMPSTRUCT.2015.08.080.

[162] Garrido M, Correia JR, Keller T, Branco FA. Connection systems between composite sandwich floor panels and load-bearing walls for building rehabilitation. Eng Struct 2016;106:209–21. https://doi.org/10.1016/j.engstruct.2015.10.036.

[163] Cen B, Liu Y, Zeng Z, Wang J, Lu X, Zhu X. Mechanical behavior of novel GFRP foam sandwich adhesive joints. Compos B Eng 2017;130:1–10. https://doi.org/10.1016/j.compositesb.2017.07.034.

[164] Marques EAS, Da Silva LFM, Flaviani M. Testing and simulation of mixed adhesive joints for aerospace applications. Compos B Eng 2015;74:123–30. https://doi.org/10.1016/j.compositesb.2015.01.005.

[165] Luo H, Yan Y, Zhang T, Liang Z. Progressive failure and experimental study of adhesively bonded composite single-lap joints subjected to axial tensile loads. J Adhes Sci Technol 2016;30:894–914. https://doi.org/10.1080/01694243.2015.1131806.

[166] Pinto AMG, Ribeiro NFQR, Campilho RDSG, Mendes IR. Effect of adherend recessing on the tensile strength of single lap joints. J Adhes 2014;90:649–66. https://doi.org/10.1080/00218464.2013.766132.

[167] Moya-Sanz EM, Ivañez I, Garcia-Castillo SK. Effect of the geometry in the strength of single-lap adhesive joints of composite laminates under uniaxial tensile load. Int J Adhesion Adhes 2017;72:23–9. https://doi.org/10.1016/j.ijadhadh.2016.10.009.

[168] Ribeiro FMF, Campilho RDSG, Carbas RJC, da Silva LFM. Strength and damage growth in composite bonded joints with defects. Compos B Eng 2016;100:91–100. https://doi.org/10.1016/j.compositesb.2016.06.060.

[169] Xu W, Wei Y. Strength analysis of metallic bonded joints containing defects. Comput Mater Sci 2012;53:444–50. https://doi.org/10.1016/j.commatsci.2011.09.008.

[170] Engerer JD, Sancaktar E. The effects of partial bonding in load carrying capacity of single lap joints. Int J Adhesion Adhes 2011;31:373–9. https://doi.org/10.1016/j.ijadhadh.2011.01.009.

[171] Banea MD, Rosioara M, Carbas RJC, da Silva LFM. Multi-material adhesive joints for automotive industry. Compos B Eng 2018;151:71–7. https://doi.org/10.1016/j.compositesb.2018.06.009.

[172] Ribeiro TEA, Campilho RDSG, da Silva LFM, Goglio L. Damage analysis of composite-aluminium adhesively-bonded single-lap joints. Compos Struct 2016; 136:25–33. https://doi.org/10.1016/j.compstruct.2015.09.054.

[173] Alves DL, Campilho RDSG, Moreira RDF, Silva FJG, Silva LFM, da Silva LFM. Experimental and numerical analysis of hybrid adhesively-bonded scarf joints. Int J Adhesion Adhes 2018;83:87–95. https://doi.org/10.1016/j.ijadhadh.2018.05.011.

[174] Avgoulas EI, Sutcliffe MPF. Biomimetic-inspired CFRP to perforated steel joints. Compos Struct 2016;152:929–38. https://doi.org/10.1016/j.compstruct.2016.06.014.

[175] Sadowski T, Kneć M, Golewski P. Spot welding-adhesive joints: modelling and testing. J Adhes 2014;90:346–64. https://doi.org/10.1080/00218464.2013.766599.

[176] Campilho RDSG, Pinto AMG, Banea MD, Da Silva LFM. Optimization study of hybrid spot-welded/bonded single-lap joints. Int J Adhesion Adhes 2012;37: 86–95. https://doi.org/10.1016/j.ijadhadh.2012.01.018.

[177] de Almeida FJS, Campilho RDSG, Silva FJG. Strength prediction of T-peel joints by a hybrid spot-welding/adhesive bonding technique. J Adhes 2018;94:181–98. https://doi.org/10.1080/00218464.2016.1244013.

[178] Sadowski T, Golewski P, Kneć M. Experimental investigation and numerical modelling of spot welding-adhesive joints response. Compos Struct 2014;112: 66–77. https://doi.org/10.1016/j.compstruct.2014.01.008.

[179] El Zaroug M, Kadioglu F, Demiral M, Saad D. Experimental and numerical investigation into strength of bolted, bonded and hybrid single lap joints: effects of adherend material type and thickness. Int J Adhesion Adhes 2018;87:130–41. https://doi.org/10.1016/j.ijadhadh.2018.10.006.

[180] Moës N, Dolbow J, Belytschko T. A finite element method for crack growth without remeshing. Int J Numer Methods Eng 1999;46:131–50. https://doi.org/10.1002/(SICI)1097-0207(19990910)46:1<131::AID-NME726>3.0.CO;2-J.

[181] Melenk JM, Babuška I. The partition of unity finite element method: basic theory and applications. Comput Methods Appl Mech Eng 1996;139:289–314. https://doi.org/10.1016/S0045-7825(96)01087-0.

[182] Xará JTS, Campilho RDSG. Strength estimation of hybrid single-L bonded joints by the eXtended Finite Element Method. Compos Struct 2017;183:397–406. https://doi.org/10.1016/j.compstruct.2017.04.009.

[183] Machado RMD, Campilho RDSG, Rocha RJB. Extended finite element modelling of aluminium stepped-adhesive joints. J Adhes 2019;00:1–24. https://doi.org/10.1080/00218464.2018.1548966.

[184] Campilho RDSG, Banea MD, Chaves FJP, Silva LFMD. eXtended Finite Element Method for fracture characterization of adhesive joints in pure mode i. Comput Mater Sci 2011;50:1543–9. https://doi.org/10.1016/j.commatsci.2010.12.012.

[185] Campilho RDSG, Banea MD, Da Silva LFM. Tensile behaviour of a structural adhesive at high temperatures by the extended finite element method. J Adhes 2013;89:529–47. https://doi.org/10.1080/00218464.2013.768106.

[186] Santos TF, Campilho RDSG. Numerical modelling of adhesively-bonded double-lap joints by the eXtended Finite Element Method. Finite Elem Anal Des 2017; 133:1–9. https://doi.org/10.1016/j.finel.2017.05.005.

[187] Stein N, Dölling S, Chalkiadaki K, Becker W, Weißgraeber P. Enhanced XFEM for crack deflection in multi-material joints. Int J Fract 2017;207:193–210. https://doi.org/10.1007/s10704-017-0228-9.

[188] Tsai CL, Guan YL, Ohanehi DC, Dillard JG, Dillard DA, Batra RC. Analysis of cohesive failure in adhesively bonded joints with the SSPH meshless method. Int J Adhesion Adhes 2014;51:67–80. https://doi.org/10.1016/j.ijadhadh.2014.02.009.

[189] Bodjona K, Lessard L. Nonlinear static analysis of a composite bonded/bolted single-lap joint using the meshfree radial point interpolation method. Compos Struct 2015;134:1024–35. https://doi.org/10.1016/j.compstruct.2015.08.136.

[190] Mubashar A, Ashcroft IA. Comparison of cohesive zone elements and smoothed particle hydrodynamics for failure prediction of single lap adhesive joints. J Adhes 2017;93:444–60. https://doi.org/10.1080/00218464.2015.1081819.